universität wien

MASTERARBEIT / MASTER'S THESIS

Titel der Masterarbeit / Title of the Master's Thesis

„Numerical Methods for the Wave Equation“

verfasst von / submitted by

Pt. Alexandros Angelakis

angestrebter akademischer Grad / in partial fulfilment of the requirements for the degree of

Master of Science (MSc)

Wien, 2021 / Vienna 2021

Studienkennzahl lt. Studienblatt / Degree programme as it appears on the student record sheet	UA 066 821
Studienkennzahl lt. Studienblatt / Degree programme as it appears on the student record sheet	Masterstudium Mathematik
Betreut von / Supervisor:	Univ. Prof. Ilaria Perugia
Mitbetreut von / Co-Supervisor:	Dipl.-Ing. Dr.techn. Marco Zank

Abstract

This thesis considers the numerical approximation of the hyperbolic initial-boundary value problems governed by the wave equation. Such problems typically arise in acoustics, electromagnetic and fluid dynamics.

Assume that the space variable varies in a bounded domain Ω and that time take values in a positive interval $(0, T)$. A typical approach is based on a variational formulation in the space variable only, set in a subspace of the Sobolev space $H^1(\Omega)$. Then the discretization consist of a conforming finite element method for the spatial variable and a second-order central difference method for the temporal variable.

An alternative approach is based on a space-time variational formulation in the bounded space-time cylinder $Q = \Omega \times (0, T)$, defined in a subspace of the Sobolev space $H^1(Q)$. Then the discretization consist of a conforming space-time finite element method.

The aforementioned methods are compared in terms of stability properties and error estimates. Numerical examples, confirming the theory, are provided.

Zusammenfassung

Diese Arbeit befasst sich mit der numerischen Approximation der Lösungen von hyperbolischen Anfangsrandwertproblemen. Ein prominenter Vertreter dieser Probleme ist die Wellengleichung und typischerweise treten solche in der Akustik, Elektromagnetik und Fluiddynamik auf.

Es wird angenommen, dass die Ortsvariable in einem beschränkten Gebiet Ω variiert und dass die Zeit positive Werte aus einem Intervall $(0, T)$ annimmt. Der klassische Ansatz basiert auf einer Variationsformulierung im Ort, die in einem Unterraum des Sobolevraums $H^1(\Omega)$ betrachtet wird. Deren Diskretisierung setzt sich aus einer konformen Finite-Elemente-Methode für die räumliche Variable und einer Finite-Differenzen-Methode für die zeitliche Variable zusammen.

Ein alternativer Ansatz basiert auf einer Raum-Zeit-Variationsformulierung im beschränkten Raum-Zeit-Zylinder $Q = \Omega \times (0, T)$, welche in einem Unterraum des Sobolevraums $H^1(Q)$ formuliert wird. Die Diskretisierung besteht aus einer konformen Raum-Zeit-Finite-Elemente-Methode.

Die erwähnten Methoden werden hinsichtlich ihrer Stabilitätseigenschaften und Fehlerabschätzungen verglichen. Abschließend werden numerische Beispiele, die die Theorie bestätigen, bereitgestellt.

Acknowledgements

There are so many people to recognize here. First and foremost, I want to thank my supervisors Ms. Univ. Prof. Ilaria Perugia and Mr. Dipl.-Ing. Dr.techn. Marco Zank for their advises, material support, critical comments and constructive suggestions throughout the coarse of my thesis work. Another big thanks goes to my friends, Eftychia, Viktor, Katerina Alexandros, Panagiota and Christina for all the emotional breakdowns you helped me survive throughout my master studies. I also want to thank my parents and grandmothers for allowing me the oppurtinity to make it this far and always giving a strong shoulder to lean on. Last but not least, I want to dedicate this master thesis to my brother, who is always by my side.

ΟΣ ΤΑ ΚΛΕΙΝ΄ ΑΙΝΙΓΜΑΤ΄ ΗΙΔΕΙ
ΚΑΙ ΚΡΑΤΙΣΤΟΣ ΗΝ ΑΝΗΡ
Oedipus Rex by Sophocles

Contents

Chapter 1

Introduction

Mathematics has always been interested in describing phenomena that are subject to changes. One of these phenomena is the propagation of waves, which are everywhere around us, from tsunamis to light to sound. Even particles can be modeled by waves. The solution of wave propagation problems is important in many areas of engineering and science, such as geophysics (seismic imaging), aerospace (radar), telecommunication (antenna design), medicine (medical imaging) and more.

In the past centuries, the motivation to study these problems has led to the development of a powerful tool, in order to efficiently describe dynamical behaviour, and has become a rich mathematical field: differential equations (DEs). More specifically, there are two types of DEs.

The first one is described by ordinary differential equations (ODEs), which contains one or more functions of one independent variable and the derivatives of those.

The second one is governed by partial differential equations (PDEs), which allows for simultaneous spatial and temporal dependencies and imposes relations between the various partial derivatives of a multi variable function. PDEs originated from the study of surfaces in geometry and a wide variety of problems in mechanics. Numerous famous mathematicians, such as Jean D'Alembert (1717-1783), Leonhard Euler (1707-1783), Joseph-Louis Lagrange (1736-1813), Piere-Simon Laplace (1749-1827) and more, became actively involved in the investigation of problems presented by PDEs.

One of the fundamental PDEs is the wave equation. The wide range of its application has led to the development of various computational techniques that attempts to approximate its solution.
In this thesis, some of these techniques are discussed.

In order to approximate the solutions to the wave equation, one needs to discretize the spatial and temporal variables. This can be done by first performing a spatial only discretization, for example by using the finite element method (FEM). FEMs have demonstrated their strong capability for approximate solutions to PDEs, see [32, 20]. The essential feature of

the space discretization is to transform the partial differential equation into a set of ordinary differential equations, which then can be discretized again on the temporal variable with finite difference methods (FDM), one of the simplest and oldest method to solve differential equations, see [5, 25]. These schemes are the most popular, because they generate cheap in memory and highly scalable algorithms. Nevertheless, for stability purposes, the time step is restricted by the spatial mesh size (CFL condition). As a consequence, the presence of small spatial elements can make the maximal value of the time step required by the CFL condition so small that the computational cost become prohibitive.

Another way to approximate solutions of the wave equation are the space-time methods, which allow for discretizations in time and space simultaneously. In this approach, the temporal variable is considered as just another spatial variable and then one addresses the problem in one dimension higher. A simply way to do that, is to use a standard finite element discretization in space combined with time. This leads to a discretization scheme, where the space-time domain is decomposed by tensor-product space-time elements, see [3, 4, 12, 15]. Space-time methods have the advantage that they provide more resources for an adaptive mesh refinement and numerical upscaling, space-time parallelisation, when the parallelization in space gets saturated, and treatment of moving boundaries. The computational cost is the main disadvantage, because a global linear system must be solved at once. Also, the production of the mesh becomes much more complicated, since one needs to mesh domains of one dimension higher.

The organization of the this thesis is as follows.

Chapter 2 introduces the essential mathematical background. Section 2.1 defines the function spaces that are used throughout the thesis, Section 2.2 states the d'Alembert method, an elemental solution of the wave equation, Section 2.3 outlines the "d+1" dimensional boundary value problem and Section 2.4 presents the variational formulation of the wave equation.

Chapter 3 contains the methods where the spatial and temporal variables are discretized separately. Section 3.1 shows the space discretization by using the finite element method, Section 3.2 outlines the finite difference method and the time discretization. Section 3.3 and Section 3.4 derive the Leapfrog and Crank-Nicolson methods respectively, and the theory of their discrete energy, stability and error estimates.

In Chapter 4, the theory of space-time methods is introduced, where, more precisely, Section 4.1 derives the variational formulation, Section 4.2 covers the space-time discretization and Section 4.3 covers the Petrov-Galerkin method and its comparison with the Newmark method.

In Chapter 5, all the numerical results for the Leapfrog, Crank-Nicolson and Petrov-Galerkin methods are presented.

Finally, Chapter 6 summarizes the thesis and proposes some directions for future investiga-

tion.

Chapter 2

The Wave Equation

The standard wave equation for a scalar function $u = u(x_1, ..., x_n, t)$ of a time variable $t \in \mathbb{R}$ and $x = (x_1, ..., x_d), x \in \mathbb{R}^d$ is

$$-\frac{1}{c^2}\partial_{tt}u + \Delta u = 0. \tag{2.1}$$

Equation (2.1) is a second-order and linear hyperbolic partial differential equation. The coefficient c is fixed non-negative and real. Note that if $c \to \infty$, then it becomes the Laplace's equation.

The wave equation is one of the most fundamental partial differential equation and it arises in many physical situations. In one dimension, it models the vibration of a string. In two dimensions, it models the vibrations of a thin membrane. In three dimensions, it models the pressure vibration of an acoustic wave in the air. The constant c represents the speed propagation for the vibrations.

The above are just some examples. There exist many additional applications of the wave equation in physics, such as the study of sound and light waves, see [8, 25, 30]. In fact, the wave equation is ubiquitous in a significant class of dynamical situation.

2.1 Elements of Function Spaces

Let $a = (a_1, ..., a_d) \in \mathbb{N}_0^d$, $|a| = a_1 + ... + a_d$ and

$$D^a = \partial_{x_1}^{a_1} ... \partial_{x_d}^{a_d}. \tag{2.2}$$

1) Space of continuous functions

- Suppose $k \in \mathbb{N}$, Ω open set in $\mathbb{R}^d$.
  $C^k(\Omega)$ is the set of all real-valued functions defined on Ω such that $D^a u$ is continuous and bounded in Ω for all $a \in \mathbb{N}_0^d$ with $|a| \leq k$ and the norm is given by

$$||u||_{C^k(\Omega)} = \sum_{|a| \leq k} \sup_{x \in \Omega} |D^a u(x)|.$$

- Suppose $k \in \mathbb{N}$, Ω open bounded set in $\mathbb{R}^d$.
  $C^k(\overline{\Omega})$ is the set of all functions $u \in C^k(\Omega)$ such that $D^a u$ can be extended to a continuous function on $\overline{\Omega}$ for all $a \in \mathbb{N}_0^d$ with $|a| \leq k$ and the norm is given by
  $$||u||_{C^k(\overline{\Omega})} = \sum_{|a| \leq k} \sup_{x \in \Omega} |D^a u(x)|.$$
- Define the support of $u \in C^0(\Omega)$: $\operatorname{supp} u$ = closure of $\{x \in \Omega : u(x) \neq 0\}$.
  Suppose $k \in \mathbb{N}$, Ω open set in $\mathbb{R}^d$.
  $C_0^k(\Omega)$ is the set of functions $u \in C^k(\Omega)$ with support bounded and contained in Ω.

Remark 2.1.1. *It holds true that for $k \in \mathbb{N}$ and Ω open set in $\mathbb{R}^d$:*
$$C_0^\infty(\Omega) = \bigcap_{k \geq 0} C_0^k(\Omega).$$

2) Space of (Lebesgue-) integrable function

- Suppose $p \in [1, \infty)$, Ω open set in $\mathbb{R}^d$.
  $L^p(\Omega)$ is the set of all measurable functions defined in Ω such that $\int_\Omega |u(x)|^p dx < \infty$ and the norm is given by
  $$||u||_{L^p(\Omega)} = (\int_\Omega |u(x)|^p dx)^{\frac{1}{p}}.$$
- $L^\infty(\Omega)$ is the set of all measurable functions defined in Ω such that, there exist $M > 0 : |u(x)| \leq M$ almost everywhere in Ω and the norm is given by
  $$||u||_{L^\infty(\Omega)} = \sup_{x \in \Omega} |u(x)|.$$
- Suppose Ω open set in $\mathbb{R}^d$.
  $L^1_{\text{loc}}(\Omega)$ is the set of all measurable functions $u \in L^1(K)$ for all compact $K \subset \Omega$.

Remark 2.1.2. *Every L^p space is a subspace of L^1_{loc} for all $p \geq 1$.*

Remark 2.1.3. *It holds that for all $p \in [1, \infty]$, $L^p(\Omega)$ is a Banach space. Moreover $L^2(\Omega)$ is a Hilbert space.*
The L^2-inner product of two real functions f and g on a measure space Ω with respect to the measure μ is given by
$$\langle f, g \rangle_{L^2(\Omega)} = \int_\Omega f \cdot g d\mu.$$

3) Sobolev spaces

- Let $\Omega \subset \mathbb{R}^d$ be a bounded Lipchitz domain, $k \in \mathbb{N}$, $1 \leq p \leq \infty$.
  The Sobolev space $W^{k,p}(\Omega)$ is defined to be the set of all functions f on Ω such that for every multi-index a with $|a| \leq k$, the mixed partial derivative exist in the weak sense and in $L^p(\Omega)$:
  $$W^{k,p}(\Omega) = \{u \in L^p(\Omega) : D^a u \in L^p(\Omega) \quad \text{for all } \ |a| \leq k\}.$$

The corresponding norms are given by

$$||u||_{W^{k,p}(\Omega)} = (\sum_{|a|\leq k} ||D^a u||^p_{L^p(\Omega)})^{\frac{1}{p}} \qquad \text{for} \quad 1 \leq p < \infty,$$

$$||u||_{W^{k,\infty}(\Omega)} = \sum_{|a|\leq k} ||D^a u||_{L^\infty(\Omega)} \qquad \text{for} \quad p = \infty.$$

Additionally, the seminorms are defined as

$$|u|_{W^{k,p}(\Omega)} = (\sum_{|a|=k} ||D^a u||^p_{L^p(\Omega)})^{\frac{1}{p}} \qquad \text{for} \quad 1 \leq p < \infty,$$

$$|u|_{W^{k,p}(\Omega)} = \sum_{|a|=k} ||D^a u||_{L^\infty(\Omega)} \qquad \text{for} \quad p = \infty.$$

Theorem 2.1.4.
For each $k \in \mathbb{N}$ and $1 \leq p \leq \infty$, the Sobolev space $W^{k,p}(\Omega)$ is a Banach space.

Proof. See [1, 10]. □

Remark 2.1.5. *Sobolev spaces with $p = 2$ form a Hilbert space $W^{k,2}(\Omega) = H^k(\Omega)$, which is a vector space with inner product in terms of the $L^2(\Omega)$ inner product:*

$$\langle u, v\rangle_{H^k(\Omega)} = \sum_{|a|\leq k} \langle D^a u, D^a v\rangle_{L^2(\Omega)} \qquad \textit{for all } u, v \in H^k(\Omega).$$

- The space $H^1_0(\Omega)$ is defined to be the closure of every function $u \in C^\infty_0(\Omega)$ in the $H^1(\Omega)$ norm

$$||u||_{H^1(\Omega)} = \left(\int_\Omega |u|^2 + |\nabla u|^2 \right)^{\frac{1}{2}}.$$

In other words $H^1_0(\Omega)$ is the set of all functions $u \in H^1(\Omega)$ such that u is the limit in $H^1(\Omega)$ of a sequence $(u_n)_{n\geq 1} \subset C^\infty_0(\Omega)$.

4) Bochner spaces

Let H be a separable real Hilbert space with inner product $\langle \cdot, \cdot \rangle_H$ and let $\Omega_1 \subset \mathbb{R}^{d_1}$ and $\Omega_2 \subset \mathbb{R}^{d_2}$ be bounded Lipschitz domains with $d_1, d_2 \in \mathbb{N}$.

- Consider the Bochner space $L^2(\Omega_1; H)$ of classes of measurable vector-valued functions $u : \Omega_1 \to H$, i.e. for each element $u \in L^2(\Omega_1; H)$, it holds true that

$$u(y) \in H \quad \text{ for almost all } y \in \Omega_1$$

such that

$$||u||_{L^2(\Omega_1;H)} = \sqrt{\int_{\Omega_1} ||u(y)||^2_H dy} < \infty.$$

Remark 2.1.6. *The Bochner space $L^2(\Omega_1; H)$ is a Hilbert space with respect to the inner product*

$$\langle u, v\rangle_{L^2(\Omega_1;H)} = \int_{\Omega_1} \langle u(y), v(y)\rangle_H dy.$$

The dual space $[L^2(\Omega_1;H)]'$ and the Bochner space $L^2(\Omega_1;H')$ are isometric, see [14, Corollary 1.3.22].

- For $k \in \mathbb{N}_0$, the Bochner Sobolev space is defined by
$$H^k(\Omega_1;H) = \{u \in L^2(\Omega_1;H) : \partial_y^\alpha u \in L^2(\Omega_1;H) \quad \text{for } |\alpha| \le k\},$$
where ∂_y is the distributional derivative on Ω_1 with respect to y for vector-valued functions and $\alpha = (\alpha_1, .., \alpha_{d_1})$ is a multi-index with the inner product
$$\langle u, v\rangle_{H^k(\Omega_1;H)} = \int_{\Omega_1} \langle u(y), v(y)\rangle_H dy + \sum_{|\alpha|\le k} \int_{\Omega_1} \langle \partial_y^\alpha u(y), \partial_y^\alpha v(y)\rangle_H dy$$
for $u, v \in H^k(\Omega_1;H)$.

Remark 2.1.7. *The Bochner Sobolev space $H^k(\Omega_1;H)$ is a Hilbert space.*

Remark 2.1.8. *For $k = 1$ and $\Omega_1 = (0,T)$, the Sobolev embedding theorem, see [21, Proposition 2.46], holds true, i.e.*
$$H^1(0,T;H) \subset C([0,T];H)$$
with a continuous embedding. Therefore, see [33, Section 2.4],
$$H^1_{0,}(0,T;H) = \{v \in H^1(0,T;H) : v(0) = 0 \quad \text{in } H\},$$
$$H^1_{,0}(0,T;H) = \{v \in H^1(0,T;H) : v(T) = 0 \quad \text{in } H\}$$
are closed subspaces of $H^1(0,T;H)$.

- The anisotropic Sobolev spaces are defined for $0 \le r \in \mathbb{R}$, $0 \le s \in \mathbb{R}$ as
$$H^{r,s}(\Omega_2 \times \Omega_1) = L^2(\Omega_1; H^r(\Omega_2)) \cap L^2(\Omega_2; H^s(\Omega_1)) \subset L^2(\Omega_2 \times \Omega_1),$$
where $L^2(\Omega_2 \times \Omega_1) \simeq L^2(\Omega_1; L^2(\Omega_2)) \simeq L^2(\Omega_2; L^2(\Omega_1))$, see [27, Theorem II.10], with the inner product
$$\langle u, v\rangle_{H^{r,s}(\Omega_2\times\Omega_1)} = \int_{\Omega_1} \langle u(\cdot, y), v(\cdot, y)\rangle_{H^r(\Omega_2)} dy + \int_{\Omega_2} \langle u(x,\cdot), v(x,\cdot)\rangle_{H^s(\Omega_1)} dx.$$

2.2 d'Alembert's Method

The one dimensional wave equation
$$\partial_{tt} u = c^2 \partial_{xx} u \tag{2.3}$$
where $u = u(x,t), x \in \mathbb{R}, t \in (0,T)$ and c constant, was solved exactly by d'Alembert (1717-1783), see [23, 5]. To illustrate the idea, introduce the coordinates (ξ, η) using the transformation:
$$\xi = x - ct, \qquad \eta = x + ct. \tag{2.4}$$
Now write
$$\partial_{xx} u = \partial_{\xi\xi} u + 2\partial_{\xi\eta} u + \partial_{\eta\eta} u, \qquad \frac{1}{c^2}\partial_{tt} u = \partial_{\xi\xi} u - 2\partial_{\xi\eta} u + \partial_{\eta\eta} u.$$
So equation (2.3) becomes
$$\partial_\xi \partial_\eta u = 0. \tag{2.5}$$

This means that u stays constant along the curves (2.4). Also, the derivative $\frac{\partial u}{\partial \xi}$ does not depend on η, i.e.

$$\partial_\eta \partial_\xi = 0 \Leftrightarrow \partial_\xi = f(\xi),$$

where f is an arbitrary function.

After integrating with respect to ξ

$$u(\xi, \eta) = F(\xi) + G(\eta),$$

where F is the primitive function of f and G is the integration "constant".

So by turning back, one can obtain the general solution of (2.3)

$$u(x,t) = F(x - ct) + G(x + ct). \tag{2.6}$$

2.3 The Initial and Boundary Value Problem

A boundary condition expresses the behaviour of the solution of the partial differential equation at the limit of the domain that the equation is defined, see [23].

Three most commonly used boundary conditions

- **Dirichlet boundary condition:**
  It determines the value of the solution u on the boundary. For example, a string fastened at two ends $x = 0$ and $x = L$ (Figure 2.1).

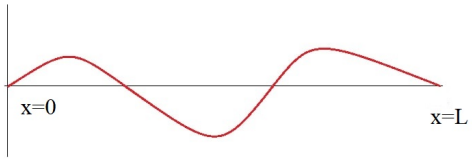

Figure 2.1

The boundary conditions are

$$u(0,t) = a(t),$$
$$u(L,t) = b(t).$$

- **Neumann boundary condition:**

  It determines the derivative of the solution u on the boundary. For example, a string that both ends can move freely in axis y (Figure 2.2).

The boundary conditions are

$$\partial_x u(0,t) = a(t),$$
$$\partial_x u(L,t) = b(t).$$

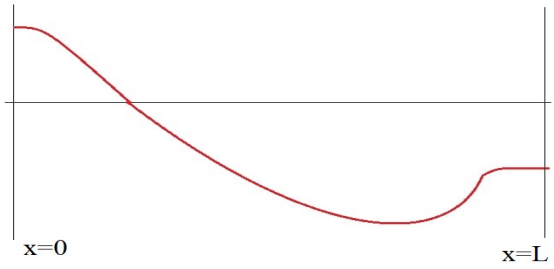

Figure 2.2

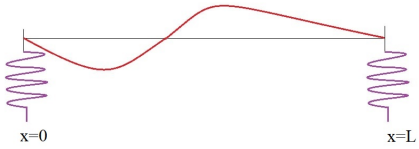

Figure 2.3

- **Robin boundary condition:**

  It constitutes the combination of the two above. For example, both ends of the strings are fastened at springs (Figure 2.3).

  The boundary conditions (as determined by the tension of the string and Hooke's Law) are

$$T\partial_x u(0,T) = ku(0,T),$$
$$T\partial_x u(L,t) = ku(L,t).$$

The partial differential equations problems can be categorized according to the conditions, to initial value problem or Cauchy problem, boundary value problem and initial boundary value problem.

Perhaps the most famous well-posed problem for the wave equation is the global Cauchy problem in $d+1$ space-time dimension:

$$-\partial_{tt}u(x,t) + c^2\Delta u(x,t) = 0, \qquad (x,t) \in \mathbb{R}^d \times \mathbb{R}, \tag{2.7}$$
$$u(x,0) = f(x), \qquad x \in \mathbb{R}^d, \tag{2.7a}$$
$$\partial_t u(x,0) = g(x), \qquad x \in \mathbb{R}^d, \tag{2.7b}$$

where f and g are the given initial data and the constant $c > 0$ is the given wave speed. For

$d = 1$, the solution of the Cauchy problem

$$\partial_{tt}u(x,t) = c^2\partial_{xx}u(x,t), \qquad (x,t) \in \mathbb{R}\times\mathbb{R}, \tag{2.8}$$
$$u(x,0) = f(x), \qquad x \in \mathbb{R}, \tag{2.8a}$$
$$\partial_t u(x,0) = g(x), \qquad x \in \mathbb{R}. \tag{2.8b}$$

is derived. For this purpose, it needs to express the arbitrary functions F and G from (2.6) in terms of the initial data f, g. Using the relation

$$\partial_t F(x-ct) = -cF'(x-ct),$$

where $F'(x-ct) = \partial_\xi F(\xi)$, the initial conditions give

$$u(x,0) = F(x) + G(x) = f(x), \tag{2.9}$$
$$\partial_t u(x,0) = c(-F'(x) + G'(x)) = g(x). \tag{2.10}$$

By solving in terms of $F'(x)$ and $G'(x)$, it follows that

$$F'(x) = \frac{1}{2}(f'(x) - \frac{1}{c}g(x)),$$
$$G'(x) = \frac{1}{2}(f'(x) + \frac{1}{c}g(x)).$$

Hence,

$$F(x) = \frac{1}{2}f(x) - \frac{1}{2c}\int_0^x g(y)dy + c_1,$$
$$G(x) = \frac{1}{2}f(x) + \frac{1}{2c}\int_0^x g(y)dy - c_1,$$

where c_1 is the integration constant chosen such that (2.9) holds.

Theorem 2.3.1. ***(d'Almbert's formula)***
Assume that $f \in C^2(\mathbb{R})$ and $g \in C^1(\mathbb{R})$. Then the unique solution $u(x,t)$ to (2.8) with (2.8a),(2.8b) satisfies $u \in C^2([0,\infty)\times\mathbb{R})$ and is represented by d'Alembert's formula:

$$u(x,t) = \frac{1}{2}(f(x+ct) + f(x-ct)) + \frac{1}{2}\int_{x-ct}^{x+ct} g(z)dz. \tag{2.11}$$

Remark 2.3.2. *Equation (2.11) illustrates the finite speed propagation property associated to the wave equation, see [23]. More precisely, the value of the solution at (x,t) is only influenced by the "initial data interval" $\{(0,y)|\ x-t \le y \le x+t\}$. That means that any changes to the initial data (2.8a)-(2.8b) outside of this interval have no effect on the solution at (x,t).*

Theorem 2.3.1 can be extended to the following initial and homogeneous Dirichlet boundary conditions. Let $c = 1$:

Corollary 2.3.3.
Let $f \in C^2([0,\infty))$, $g \in C^1([0,\infty))$, and assume that $f(0) = g(0) = 0$. Then the unique

solution to the following "1+1" dimensional initial boundary value problem

$$-\partial_{tt}u(x,t)+\partial_{xx}u(x,t)=0, \qquad (x,t)\in(0,\infty)\times(0,\infty), \tag{2.12}$$
$$u(0,t)=0, \qquad t\in[0,\infty), \tag{2.12a}$$
$$u(x,0)=f(x), \qquad x\in(0,\infty), \tag{2.12b}$$
$$\partial_t u(x,0)=g(x), \qquad x\in(0,\infty), \tag{2.12c}$$

satisfies $u\in C^2([0,\infty)\times[0,\infty))$. *Furthermore, it can be represented as*

$$u(x,t)=\begin{cases}\frac{1}{2}(f(x+t)+f(x-t)+\frac{1}{2}\int_{z=|x-t|}^{z=x+t}g(z)dz, & \text{if } 0\le t\le x\\ \frac{1}{2}(f(x+t)-f(t-x))+\frac{1}{2}\int_{z=|x-t|}^{z=x+t}g(z)dz, & \text{if } 0\le x\le t.\end{cases} \tag{2.13}$$

Proof. The idea is to extend u to be odd in x and reduce the problem to the case of Theorem 2.3.1. Define

$$\bar{u}(x,t)=\begin{cases}u(x,t) & \text{if } t\ge 0, x\ge 0,\\ -u(-x,t) & \text{if } t\ge 0, x<0,\end{cases} \tag{2.14}$$

$$\begin{aligned}\bar{f}(x)&=\begin{cases}f(x) & \text{if } x\ge 0,\\ -f(-x) & \text{if } x<0,\end{cases}\\ \bar{g}(x)&=\begin{cases}g(x) & \text{if } x\ge 0,\\ -g(-x) & \text{if } x<0.\end{cases}\end{aligned} \tag{2.15}$$

Since $u(x,t)$ solves (2.12), it follows that $\bar{u}(x,t)$ is a solution to (2.8) for $c=1$ and $(x,t)\in\mathbb{R}\times\mathbb{R}$ with initial data

$$\bar{u}(x,0)=\bar{f}(x), \qquad \partial_t\bar{u}(x,0)=\bar{g}(x).$$

Thus, by (2.11)

$$\bar{u}(x,t)=\frac{1}{2}(\bar{f}(x+t)+\bar{f}(x-t))+\frac{1}{2}\int_{z=x-t}^{z=x+t}\bar{g}(z)dz. \tag{2.16}$$

The expression (2.13) easily follows from considering (2.17) separately in the space-time regions $\{(x,t)|\ 0\le t\le x\}$ and $\{(x,t)|\ 0\le x\le t\}$ and from definitions (2.14), (2.15).
Note that in the case $\{(x,t)|\ 0\le t\le x\}$, since $\bar{g}$ is odd, the part of the integral from $x-t$ to $t-x$ cancels and thus the only contribution comes from the integration interval $[|x-t|,x+t]$. □

2.4 Variational Formulation

Let $\Omega\subset\mathbb{R}^d$ be a bounded Lipschitz domain and $T>0$ be a given terminal time. Consider the initial boundary value problem for the wave equation

$$\partial_{tt}u(x,t)-c(x)^2\Delta u(x,t)=f(x,t), \qquad (x,t)\in\Omega\times(0,T), \tag{2.17}$$
$$u(x,t)=0, \qquad (x,t)\in\partial\Omega\times[0,T], \tag{2.17a}$$
$$u(x,0)=u_0(x), \qquad x\in\Omega, \tag{2.17b}$$
$$\partial_t u(x,0)=u_1(x), \qquad x\in\Omega, \tag{2.17c}$$

where the function $u : \Omega \times (0,T) \to \mathbb{R}$ is sought, the right-hand side $f : \Omega \times (0,T) \to \mathbb{R}$ is given, $u_0, u_1 : \Omega \to \mathbb{R}$ are the given initial conditions and $c : \Omega \to \mathbb{R}$ is the given wave speed. Define $V = H_0^1(\Omega)$ and

$$Lu(x,t) := -c(x)^2 \Delta u(x,t). \tag{2.18}$$

The operator L is formally self-adjoint. The variational setting of (2.17) with (2.17a)-(2.17c), see [16, 23], is

$$\partial_{tt} u + Lu = f \qquad \text{in } V', \text{a. e. in } (0,T), \tag{2.19}$$
$$u = 0 \qquad \text{on } \partial\Omega, \text{a.e. in } (0,T), \tag{2.19a}$$
$$u(0) = u_0 \qquad \text{in } \Omega, \tag{2.19b}$$
$$\partial_t u(0) = u_1 \qquad \text{in } \Omega. \tag{2.19c}$$

In order to formulate a definition of a weak solution, let $a : H_0^1(\Omega) \times H_0^1(\Omega) \to \mathbb{R}$ be the bilinear form associated with (2.18) given by

$$a(u,v) = \int_\Omega c(x)^2 \nabla_x u(x) \cdot \nabla_x v(x) dx \tag{2.20}$$

for $u, v \in H_0^1(\Omega)$.

Assumptions 2.4.1.
The following holds true:

- *The wave speed c(x) satisfies*
$$c \in C^\infty(\overline{\Omega})$$
and $\exists c_0 > 0 : \forall x \in \overline{\Omega} : \ c_0 \leq c(x)$.
- *The set* $\Omega \subseteq \mathbb{R}^d$ *is bounded Lipschitz domain,* $T > 0$, $f \in L^2(0,T; L^2(\Omega))$, $u_0 \in H_0^1(\Omega)$ *and* $u_1 \in L^2(\Omega)$.

Lemma 2.4.2.
The following holds true:

- $a(u,v) = a(v,u)$ *is a symmetric bilinear form on* $H_0^1(\Omega)$.
- *There exist constants* $C > 0$ *and* $\beta > 0$ *such that, for all* $u, v \in H_0^1(\Omega)$, $a : H_0^1(\Omega) \times H_0^1(\Omega) \to \mathbb{R}$ *is* <u>continuous</u>
$$|a(u,v)| \leq C||u||_{H^1(\Omega)}||v||_{H^1(\Omega)}$$
and it is <u>coercive</u>
$$\beta||u||^2_{H^1(\Omega)} \leq a(u,u).$$

Proof. See [16, 8]. □

Definition 2.4.3.
A function $u : [0,T] \to H_0^1(\Omega)$ *is a weak solution of* (2.19) *with* (2.19a)-(2.19c) *if:*

1. *u has weak derivatives* $\partial_t u$ *and* $\partial_{tt} u$ *and*
$$u \in C([0,T]; H_0^1(\Omega)), \quad \partial_t u \in C([0,T]; L^2(\Omega)), \quad \partial_{tt} u \in L^2(0,T; [H_0^1(\Omega)]').$$

2. *For every* $v \in H_0^1(\Omega)$

$$\langle \partial_{tt} u(t), v \rangle_\Omega + a(u(t), v) = \langle f(t), v \rangle_{L^2(\Omega)}$$

for t *almost everywhere in* $[0,T]$ *and* $a(\cdot,\cdot)$ *as defined in* (2.20)*, where* $\langle \cdot, \cdot \rangle_\Omega$ *is the duality pairing on* $V' \times V$*.*

3. $u(0) = u_0$ *and* $\partial_t u(0) = u_1$*.*

Existence of a weak solution for the wave equation can be proved via the Galerkin Method, see [8, 34, 28, 9].

Theorem 2.4.4.
For a given right-hand side and initial conditions, there exists a unique u *that solves the variational formulation* (2.19) *with* (2.19a)-(2.19c)*. Moreover the solution satisfies:*

$$\begin{aligned} u &\in L^2(0,T; H_0^1(\Omega)) \cap C([0,T]; H_0^1(\Omega)), \\ \partial_t u &\in L^2(0,T; L^2(\Omega)) \cap C([0,T]; L^2(\Omega)), \\ \partial_{tt} u &\in L^2(0,T; [H_0^1(\Omega)]'). \end{aligned}$$

The stability *estimate of the unique solution is:*

$$\sqrt{||u||^2_{L^2(0,T;H_0^1(\Omega))} + ||\partial_t u||^2_{L^2(0,T;L^2(\Omega))}} \leq C(|u_0|_{H^1(\Omega)} + ||u_1||_{L^2(\Omega)} + ||f||_{L^2(0,T;L^2(\Omega))}),$$

with a constant $C > 0$*.*
The energy equality *with* $t_1 < t_2$*,* $t_1, t_2 \in (0,T)$*:*

$$\mathcal{E}(t_2) - \mathcal{E}(t_1) = \int_{t_1}^{t_2} \langle f(s), \partial_t u(s) \rangle_{L^2(\Omega)} ds,$$

where the total energy *is given by:*

$$\mathcal{E}(t) = \frac{1}{2} ||\partial_t u(t)||^2_{L^2(\Omega)} + \frac{1}{2} ||a(u(t), u(t))||^2_{L^2(\Omega)}$$

with $t \in [0,T]$*.*

Proof. For the existence and uniqueness, see [8, 34, 28, 9]. For the regularity and energy equality, see

- [28, Korollar 12.6],
- [9, Lemma 7].

□

Chapter 3

Method of Lines for the Wave Equation

The analytical solution of the solution of the differential equations, by which various technical problems are described, is possible only in some special cases, where noises and geometrical shapes are too simple. To solve the more complex ones, approximate methods are needed and the method of finite element is one of them.

Finite Elements Methods (FEM) are computational methods for the purpose of calculation of approximate solutions to natural phenomena described through partial differential equations. It is based on the idea, that constructions are complex objects that can be separated and be broken down into smaller parts and the approximated equations can be solved more easily, see [32, 20]. Although it is an approximated method, it gives dependably results and it has the advantage that it can be used in most problems. The disadvantage is the increased computing power requirements, especially when applied to complex models, something that has been mostly overcome the last years.

It can be said that finite element method have had its origins in the work of Euler, as early in the 16th century. However, the earliest mathematical papers on it can be found in the works of Schellbach [1851] and Courant [1943]. This method was independently developed by engineers to address structural problems related to aerospace and civil engineering. The developments began in the mid-1950s with the papers of Turner, Clough, Martin and Topp [1956], John Argyris [1957], and Babuska and Aziz [1972]. The books by Zienkiewicz [1971] and Strang, and Fix [1973] also laid the foundations for future development in FEM.

3.1 Space Discretization: Finite Element Method

The finite element method is based on the assumption that each continuous function within its definition field can be approximated by a sequence of functions, that are defined on a finite number of small pieces, which all together they can cover the definition field. Inside one of these pieces the unknown function is approached in a systematic way with the help of predecided reference functions, see [20, 5, 30, 25].

Let $\Omega \subset \mathbb{R}^d$, $d = 1, 2, 3$, be a bounded Lipschitz domain. In addition Ω is an interval

for $d = 1$, polygonal for $d = 2$ or polyhedral for $d = 3$.

Definition 3.1.1.
*A **mesh** $\mathcal{T} = \{\omega_i\}_{i=1}^N$ of the domain Ω is a collection of nonoverlaping cells $\{\omega_i\}_{i=1}^N$ such that*

1. $\mathring{\omega}_i \neq \emptyset$
2. $\mathring{\omega}_i \cap \mathring{\omega}_j = \emptyset$ *for* $i \neq j$
3. $\cup_{i=1}^N \omega_i = \overline{\Omega}$
4. *Set* $F = \omega_i \cap \omega_j$ *for* $i \neq j$. *One of the following is satisfied:*
   (a) $F = \emptyset$.
   (b) F *is a node for* $d = 1$.
   (c) F *is a vertex or an entire edge shared by* ω_i *and* ω_j *for* $d = 2, 3$.

where N is the spatial discretization parameter.
The local mesh size is given as

$$h_{\omega_i} = \left(\int_{\omega_i} dx \right)^{\frac{1}{d}} \quad \text{for } i = 1, ..., N.$$

In addition,

$$h = \max_{i=1,...,N} h_{\omega_i} \quad \text{and} \quad h_{min} = \min_{i=1,...,N} h_{\omega_i}$$

are the global mesh size and minimal mesh size respectively.

Remark 3.1.2. *An ordering of the vertices is useful, to the interior vertices $\{x_i\}_{i=1}^M \subset \Omega$ and the boundary vertices $\{x_i\}_{M+1}^{\bar{M}}$, where $\bar{M}$ is the number of vertices of the decomposition $\mathcal{T}$.*

Meshes are a crucial building block in the design of the finite dimensional trial and test space, used in the finite element method and provide subdomains for integration in order to build the system matrix and vector of the right hand side of the equation, see [13].

Moreover, the orientation of geometric objects of the mesh is important for defining high orders basis function. For an edge, needs to define its direction and for a face ($d = 3$) needs to specify an ordering of the edges along the boundary.

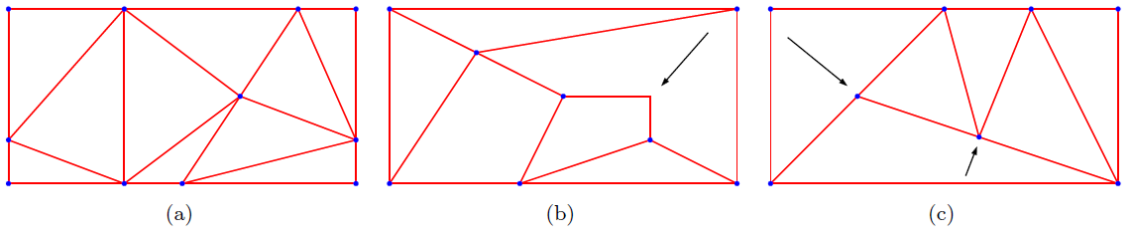

Figure 3.1: (a) Two-dimensional mesh and the set of edges (red) and nodes (blue). (b) A geometrical node is not a topological node. (c) A triangulation that is not conforming and possesses two hanging nodes.

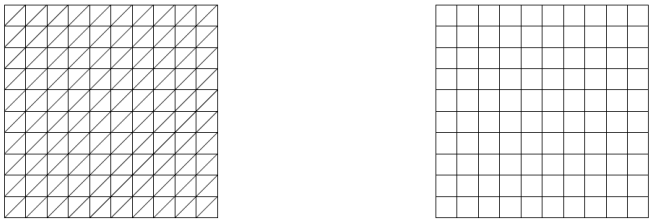

Figure 3.2: Examples of triangular and quadrilateral grids in two dimensions.

Reference Element $\hat{K}$

- For triangle: reference triangle with nodes $(0,0)$, $(1,0)$, $(1,1)$,
- for quadrilateral: reference quad $[0,1]^2$ or $[-1,1]^2$,
- for tetrahedra: reference tetrahedron with nodes $(0,0,0)$, $(1,0,0)$, $(0,1,0)$, $(0,1,0)$,
- for prism: reference prism = reference triangle $\times[0,1]$,
- for pyramid: reference pyramid with nodes $(0,0,0)$, $(1,0,0)$, $(1,1,0)$, $(0,1,0)$ and $(0.5,0.5,1)$,
- for hexahedra: reference hexahedron $[0,1]^3$.

In meshes with diffrent cell types, they can be more than one reference cell.

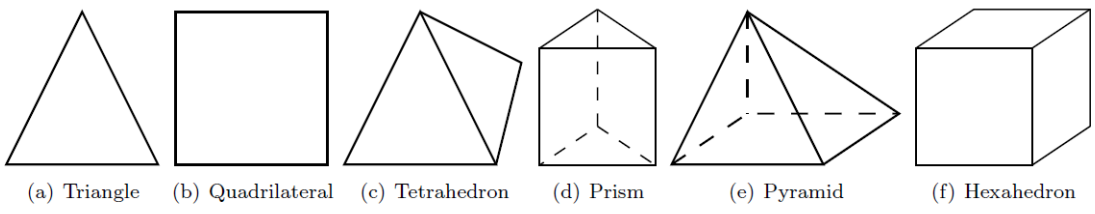

Figure 3.3: Cell types in 2D and 3D.

Definition 3.1.3.
Let K be the "physical" cell and $\hat{K}$ the reference cell. Then, there exist an affine mapping, linear and bijective from K to $\hat{K}$:

$$\Phi : \hat{K} \to K, \quad \xi \to f\xi + \mu, \quad f \in \mathbb{R}^{d\times d} \text{ regular }, \mu \in \mathbb{R}^d.$$

Basis function
Instead of searching for a solution $u \in H_0^1(\Omega)$ such that, for all test functions v in $H_0^1(\Omega)$ holds, one can search in a finite dimensional subspace of $H^1(\Omega)$. This space will consist of those functions in $H^1(\Omega)$ which are piecewise linear continuous.

Ansatz 3.1.4.
Let the space

$$S_h^1(\Omega) = \text{span}\{\psi_i\}_{i=1}^{\bar{M}} \subset H^1(\Omega),$$

where ψ_i are the nodal basis function satisfying

$$\psi_i(x_k) = \delta_{ik}, \quad i,k = 1,...,\bar{M}$$

and δ_{ik} be the Kronecker delta.
Further, let

$$S_{h,0}^1(\Omega) := \text{span}\{\psi_i\}_{i=1}^{M} = S_h^1(\Omega) \cap H_0^1(\Omega).$$

Any function $u_h \in S_{h,0}^1(\Omega)$ admits a representation

$$u_h(x) = \sum_{i=1}^{M} a_i\psi_i(x)$$

for $x \in \overline{\Omega}$ and the coefficients $a_i \in \mathbb{R}$.

Example 3.1.5. *Take the acoustic wave equation*

$$\partial_{tt}u - c^2\partial_{xx}u = f \quad \text{ in } [0,1]\times(0,T), \tag{3.1}$$

where $c \in \mathbb{R}$, $c > 0$, is the wave speed.
Create the mesh $\mathcal{T} = \{\omega_i\}_{i=1}^N$ of the domain $(0,1)$, and multiply (3.1) by an arbitrary test basis function $\psi_j \in S_{h,0}^1(0,1), \quad j = 1,...,M$ and integrate over the whole domain. After doing partial integration, it gives

$$\int_0^1 \partial_{tt}u\psi_j dx + c^2\int_0^1 \partial_x u\partial_x\psi_j dx = \int_0^1 f\psi_j dx. \tag{3.2}$$

An approximation by using the basis function

$$u(x,t) \approx u_h(x,t) = \sum_{i=1}^{M} a_i(t)\psi_i(x), \tag{3.3}$$

$$\partial_{tt}u(x,t) \approx \partial_{tt}u_h(x,t) = \partial_{tt}\sum_{i=1}^{M} a_i(t)\psi_i(x). \tag{3.4}$$

Merging together (3.2),(3.3),(3.4) gives

$$\left[\sum_{i=1}^{M}\partial_{tt}a_i(t)\int_0^1 \psi_i\psi_j dx\right] + c^2\left[\sum_{i=1}^{M} a_i(t)\int_0^1 \partial_x\psi_i\partial_x\psi_j dx\right] = \int_0^1 f\psi_j dx.$$

Define the mass matrix M_h with entries $M_h[j,i] = \int_0^1 \psi_i \psi_j dx$ for $i,j = 1,...,M$,
the stiffness matrix A_h with entries $A[j,i] = \int_0^1 \partial_x \psi_i \partial_x \psi_j dx$ for $i,j = 1,...,M$,
and the vector of the right-hand side $\underline{f}(t)$ with entries $\underline{f}(t)[j] = \int_0^1 f(.,t)\psi_j dx$ for $j = 1,...,M$.
So now the problem can be written in the Matrix form:

$$M_h \partial_{tt} \underline{a}(t) + c^2 A_h \underline{a}(t) = \underline{f}(t).$$

How to solve this time-dependent problem?

Let $\mathcal{T} = \{\omega_i\}_{i=1}^N$ be a mesh of Ω. Consider a sequence

$$(\mathcal{T}_\nu)_{\nu \in \mathbb{N}} = \{\mathcal{T}_\nu : \nu \in \mathbb{N}\}$$

of decompositions of Ω.

Definition 3.1.6.
The sequence $(\mathcal{T}_\nu)_{\nu\in\mathbb{N}}$ is called shape-regular (or regular or quasi-uniform), if there exist a constant $c_f > 0$ such that

$$\forall \nu \in \mathbb{N} : \forall \omega \in \mathcal{T}_\nu : \sup_{x,y\in\omega} |x - y| \leq c_f r_\omega,$$

where r_ω is the radius of the largest ball that can be inscribed in the spatial element $\omega \in \mathcal{T}_\nu$.
The sequence $(\mathcal{T}_\nu)_{\nu\in\mathbb{N}}$ is called globally quasi-uniform, if there exist a constant $c_g \geq 1$ such that

$$\forall \nu \in \mathbb{N} : \frac{h_{max}(\mathcal{T}_\nu)}{h_{min}(\mathcal{T}_\nu)} \leq c_g.$$

Lemma 3.1.7.
Let the sequence $(\mathcal{T}_\nu)_{\nu\in\mathbb{N}}$ of decomposition of Ω be admissible, shape-regular and globally quasi-uniform. The inverse inequality

$$\forall v_h \in S_h^1(\Omega) : |v_h|^2_{H^1(\Omega)} \leq c_{inv} h^{-2} ||v_h||^2_{L^2(\Omega)}$$

holds true for a constant $c_{inv} > 0$.

Proof. See [31, Lemma 9.8]. □

For the one dimensional case, $d = 1$, consider a function $v \in S_h^1(\omega_i)$ and

$$v(x) = v(x_{\omega_i} + \xi h_{\omega_i}) = \tilde{v}(\xi) \quad \text{for } \xi \in (0,1)$$

and obtain for the local norms of v and $\tilde{v}$

$$||\partial_x v||^2_{L^2(\omega_i)} = h^{-1} ||\partial_\xi \tilde{v}||^2_{L^2(0,1)}. \tag{3.5}$$

Let $\omega_i \in \mathbb{R}^d$ be a finite element of a shape regular and admissible decomposition $\mathcal{T}$. If v is sufficiently smooth then

$$||\partial_x v||_{L^2(\omega_i)} \leq c h^{-1}_{\omega_i} ||\partial_\xi \tilde{v}||^2_{L^2(0,1)}.$$

To compute the gradient of the linear function

$$\tilde{v}(\xi) = \sum_{k=1}^{2} v_k \psi_k(\xi),$$

one obtains

$$\partial_\xi \tilde{v} = v_2 - v_1$$

and therefore

$$||\partial_\xi \tilde{v}||^2_{L^2(\mathcal{T})} = (v_2 - v_1)^2 \leq 2[v_1^2 + v_2^2] \leq 12h^{-1}||v||^2_{L^2(\omega_i)}. \tag{3.6}$$

If the decomposition $\mathcal{T}$ is globally quasi-uniform, the (3.5) and (3.6) becomes

$$||\partial_x v||^2_{L^2(\mathcal{T}} \leq 12h^{-1}||v||^2_{L^2(\mathcal{T})},$$

see [31, (9.4), Theorem 9.3, Lemma 9.4, (9.19), pages 205-217].
So, for the one dimensional case $d = 1$, the inverse inequality constant is c_{inv}=12.

3.2 Time Discretization: Finite Difference Method

The classical finite difference approach approximates the differential operator constituting the field equation locally.
The derivatives of the partial differential equation are approximated by linear combinations of function values at the structured grid points, see [5, 25].
The following definition is for the derivatives on time.

Definition 3.2.1. *Let $t \in (0, T), N_t \in \mathbb{N}, N_t \geq 2$ be the time discretization parameter. The constant time step size is $\tau = \frac{T}{N_t} \in (0, \frac{T}{2})$ and the corresponding time steps are $t^k = k\tau$ for $k = 0, ..., N_t$.*

- *For a function $u : \Omega \times [0, T] \to \mathbb{R}$, define*
  - *the continuous first-order forward operator:*
$$D^+_\tau u(x, t) = \frac{u(x, t + \tau) - u(x, t)}{\tau}, \quad x \in \Omega, \quad t \in [0, T - \tau],$$
  - *the continuous first-order backward operator:*
$$D^-_\tau u(x, t) = \frac{u(x, t) - u(x, t - \tau)}{\tau}, \quad x \in \Omega, \quad t \in [\tau, T],$$
  - *the continuous second-order central difference operator:*
$$D^2_\tau u(x, t) = \frac{u(x, t + \tau) - 2u(x, t) + u(x, t - \tau)}{\tau^2}, \quad x \in \Omega, \quad t \in [\tau, T - \tau].$$
- *For a sequence of functions $V^k : \Omega \to \mathbb{R}$, $k = 0, ..., N_t$ define:*
  - *the discrete first-order forward operator:*
$$D^+_\tau V^k(x) = \frac{V^{k+1}(x) - V^k(x)}{\tau}, \quad x \in \Omega, \quad k \in \{0, 1, ..., N_t - 1\},$$
  - *the discrete first-order backward operator:*
$$D^-_\tau V^k(x) = \frac{V^k(x) - V^{k-1}(x)}{\tau}, \quad x \in \Omega, \quad k \in \{1, ..., N_t\},$$
  - *the discrete second-order central difference operator:*
$$D^2_\tau V^k(x) = \frac{V^{k+1}(x) - 2V^k(x) + V^{k-1}(x)}{\tau^2}, \quad x \in \Omega, \quad k \in \{1, 2, ..., N_t - 1\}.$$

Moreover, define the function $u^k : \Omega \to \mathbb{R}$ and $u : \Omega \times [0,T] \to \mathbb{R}$ such that:

$$u^k(x) = u(x,t^k), \quad x \in \Omega, \quad k \in \{0,1,...,N_t\}.$$

So the equalities

$$\begin{aligned} D_\tau^+ u(x,t^k) = (D_\tau^+ u)^k(x) &= D_\tau^+ u^k(x), \qquad x \in \Omega, \quad k \in \{0,1,...,N_t-1\}, \\ D_\tau^- u(x,t^k) = (D_\tau^- u)^k(x) &= D_\tau^- u^k(x), \qquad x \in \Omega, \qquad k \in \{1,...,N_t\}, \\ D_\tau^2 u(x,t^k) = (D_\tau^2 u)^k(x) &= D_\tau^2 u^k(x), \qquad x \in \Omega, \quad k \in \{1,2,...,N_t-1\}, \end{aligned}$$

hold true.

Example 3.2.2. *The time-dependent problem from the Example 3.1.5:*

$$M_h \partial_{tt} \underline{a}(t) + c^2 A_h \underline{a}(t) = \underline{f}(t) \quad \text{for } t \in (0,T).$$

By using the second-order central difference approximation for the time derivative, it becomes:

$$M_h \frac{\underline{a}^{k+1} - 2\underline{a}^k + \underline{a}^{k-1}}{\tau^2} + c^2 A_h \underline{a}^{k+1} = \underline{f}^k,$$

where $\underline{a}^k(t) = \underline{a}(t^k)$, $\underline{f}^k = \underline{f}(t^k)$ *with* t^k *be the corresponding time steps.*
This leads to the solution at time t^{k+1}, *with* t^k, t^{k-1} *known:*

$$\underline{a}^{k+1} = \left[M_h + c^2\tau^2 A_h\right]^{-1} (\underline{f}^k \tau^2 + M_h(2\underline{a}^k - \underline{a}^{k-1})),$$

which is easier to solve than the original equation (3.1).

3.3 Leapfrog Method for the Wave Equation

Let the wave speed of (2.17) be $c(x) = 1$ for all $x \in \Omega$. Let the sequence $(\mathcal{T}_\nu)_{\nu\in\mathbb{N}}$ be admissible, shape-regular and globally quasi-uniform, $f \in C([0,T]; L^2(\Omega))$ be the given right-hand side of (2.17), and $N_t \in \mathbb{N}, N_t \geq 2$ such that $\tau = \frac{T}{N_t} \in [0, \frac{T}{2}]$ be the constant step size with the corresponding time steps t^k given.
Applying the Leapfrog method on the equation (2.17) with (2.17a)-(2.17c), consider the approximation on the spatial variable as in Ansatz 3.1.4:

$$U^k(x) = \sum_{i=1}^{M} a_i^k \psi_i(x) \approx u(x,t^k) \quad \text{for } x \in \Omega, k = \{0,1,...,N_t\}$$

and afterwards apply the discrete second-order central difference operator for the temporal variable, see [32, 19, 2].
Find a function $U^k \in S^1_{h,0}(\Omega)$ for $k = 0,1,...,N_t$ such that

$$U^0 = u_{0,h}, \quad U^1 = u_{1,h}, \tag{3.7}$$

where $u_{0,h}$ and $u_{1,h}$ are approximations of the initial conditions (2.17b) and (2.17c):

$$u(\cdot,0) = u_0 \approx u_{0,h} \in S^1_{h,0}(\Omega), \quad u(\cdot,t^1) \approx u_{1,h} \in S^1_{h.0}(\Omega).$$

For $k = 1,...,N_t - 1$, take a test function $v_h \in S^1_{h,0}(\Omega)$ multiply and integrate on the approximated wave equation (as is being done in Example 3.1.5) and together with the second-order central difference operator on (2.17) gives:

$$\frac{1}{\tau^2}\langle U^{k+1} - 2U^k + U^{k-1}, v_h\rangle_{L^2(\Omega)} + \langle \nabla_x U^k, \nabla_x v_h\rangle_{L^2(\Omega)} = \langle f^k, v_h\rangle_{L^2(\Omega)}, \tag{3.8}$$

where $f^k(x) = f(x, t^k)$ for $x \in \Omega$ is the right-hand side f.
By changing $v_h = \psi_j$, $j = 1, ..., M$, the discrete variational formulation (3.8) is equivalent to solving the linear system:

$$M_h \underline{a}^{k+1} = \tau^2(\underline{f}^k - A_h \underline{a}^k) + M_h(2\underline{a}^k - \underline{a}^{k-1}) \tag{3.9}$$

for $k = 1, ..., N_t - 1$, where $\underline{a}^k = \begin{pmatrix} a_1^k \\ ... \\ a_M^k \end{pmatrix}$ is the unknown coefficient vector, the mass matrix $M_h \in \mathbb{R}^{M\times M}$ and stiffness matrix $A_h \in \mathbb{R}^{M\times M}$:

$$M_h[j,i] = \langle \psi_i, \psi_j \rangle_{L^2(\Omega)}, \quad A_h[j,i] = \langle \nabla_x \psi_i, \nabla_x \psi_j \rangle_{L^2(\Omega)}, \tag{3.10}$$

and $\underline{f}^k = \begin{pmatrix} \langle f^k, \psi_1 \rangle_{L^2(\Omega)} \\ ... \\ \langle f^k, \psi_M \rangle_{L^2(\Omega)} \end{pmatrix}$.

Remark 3.3.1. *In every iteration, a linear system with the mass matrix has to be solved for $\underline{a}^{k+1}$, when $\underline{a}^k$ and $\underline{a}^{k-1}$ are known. Since the mass matrix is positive definite,* (3.9) *is uniquely solvable, hence* (3.8) *has a unique solution $U^{k+1} \in S^1_{h,0}(\Omega)$ for $k = 1, ..., N_t - 1$, when U^k, U^{k-1} are known.*

Lemma 3.3.2.
The mass matrix M_h and the stiffness matrix A_h are positive definite. Furthermore, $\beta_1 M_h + \beta_2 A_h$ is positive definite for $\beta_1 > 0$, $\beta_2 > 0$.

Proof. Let $w_h(x) \in S^1_{h,0}(\Omega)$, admits a represantation

$$w_h(x) = \sum_{i=1}^{M} w_i \psi_i(x)$$

for $x \in \overline{\Omega}$ and $w_i \in \mathbb{R}$. Setting $w = (w_1, ..., w_M)^\top$ yields that

$$w^\top M_h w = \sum_{i=1}^{M}\sum_{j=1}^{M} w_i \int_\Omega \psi_i(x) \cdot \psi_j(x) dx \; w_j = \int_\Omega \sum_{i=1}^{M} w_i \psi_i(x) \cdot \sum_{j=1}^{M} w_j \psi_j(x) \; dx$$
$$= \int_\Omega |w_h(x)|^2 \geq 0$$

with equality if and only if w_h=0. Furthermore,

$$w^\top A_h w = \sum_{i=1}^{M}\sum_{j=1}^{M} w_i \int_\Omega \nabla\psi_i(x) \cdot \nabla\psi_j(x) dx \; w_j = \int_\Omega \sum_{i=1}^{M} \nabla(w_i \psi_i(x)) \cdot \sum_{j=1}^{M} \nabla(w_j \psi_j(x)) \; dx$$
$$= \int_\Omega |\nabla w_h(x)|^2 \geq 0$$

with equality if and only if $\nabla w_h(x) = 0$, that is, if w_h is constant. Since w_h is zero on the boundary by definition, it follows that the constant must be zero.
Therefore, the above expressions are equal to zero when $w_h(x) = 0$, that is, when $w = 0$. So, M_h and A_h are positive definite.
For $\beta_1 > 0$, $\beta_2 > 0$ it holds true that

$$w^\top(\beta_1 M_h)w > 0, \qquad w^\top(\beta_2 M_h)w > 0$$

for $w \neq 0$. So, it holds

$$w^\top(\beta_1 M_h + \beta_2 A_h)w = w^\top(\beta_1 M_h)w + w^\top(\beta_2 A_h)w > 0.$$

Therefore, $\beta_1 M_h + \beta_2 A_h$ is positive definite for $\beta_1 > 0$, $\beta_2 > 0$. □

Definition 3.3.3.
Let $U^k \in S^1_{h,0}(\Omega)$ be the solution of (3.7),(3.8) for time step t^k, $k = 0, ..., N_t$. The discrete energy of the Leapfrog method (3.7),(3.8) is defined by

$$\mathcal{E}^k_{\mathrm{LF}} = \frac{1}{2}||D^+_\tau U^k||_{L^2(\Omega)} + \frac{1}{2}\langle \nabla_x U^k, \nabla_x U^{k+1}\rangle_{L^2(\Omega)},$$

for $k = 0, 1, ..., N_t - 1$.

In general, $\mathcal{E}_{\mathrm{LF}}$ is not a non-negative. For the stability, it needs to determine a condition in order to be non-negative. This is called the CFL condition.

Lemma 3.3.4.
Assume that there exists $\lambda \in (0, 2)$ such that the CFL condition

$$c_{inv}\frac{\tau^2}{h^2} \leq 2 - \lambda \tag{3.11}$$

is satisfied, where c_{inv} is the constant from Lemma 3.1.7.
Then the inequality

$$\mathcal{E}^k_{\mathrm{LF}} \geq \frac{\lambda}{4}||D^+_\tau U^k||^2_{L^2(\Omega)} + \frac{1}{4}|U^{k+1}|^2_{H^1(\Omega)} + \frac{1}{4}|U^k|^2_{H^1(\Omega)}$$

holds true for $k = 0, ..., N_t - 1$.

Proof. Let $k \in \{0, ..., N_t - 1\}$.. Begin by rewriting the second term from the discrete energy on Definition 3.3.3 in terms of symmetric arguments, before applying the inverse inequality (Lemma 3.1.7) since $D^+_\tau U^k \in S^1_h(\Omega)$:

$$\begin{aligned}
2\langle \nabla_x U^k, \nabla_x U^{k+1}\rangle_{L^2(\Omega)} &= \langle \nabla_x U^{k+1}, \nabla_x U^{k+1}\rangle_{L^2(\Omega)} + \langle \nabla_x U^k, \nabla_x U^k\rangle_{L^2(\Omega)} \\
&\quad - \langle \nabla_x U^{k+1} - \nabla_x U^k, \nabla_x U^{k+1} - \nabla_x U^k\rangle_{L^2(\Omega)} \\
&= |U^{k+1}|^2_{H^1(\Omega)} + |U^k|^2_{H^1(\Omega)} - \tau^2|D^+_\tau U^k|^2_{H^1(\Omega)} \\
&\geq |U^{k+1}|^2_{H^1(\Omega)} + |U^k|^2_{H^1(\Omega)} - c_{inv}\frac{\tau^2}{h^2}||D^+_\tau U^k||^2_{L^2(\Omega)},
\end{aligned}$$

Inserting it to the discrete energy $\mathcal{E}^k_{\mathrm{LF}}$ gives:

$$\begin{aligned}
\mathcal{E}^k_{\mathrm{LF}} &\geq \frac{1}{2}\left(1 - c_{inv}\frac{\tau^2}{2h^2}\right)||D^+_\tau U^k||^2_{L^2(\Omega)} + \frac{1}{4}|U^{k+1}|^2_{H^1(\Omega)} + \frac{1}{4}|U^k|^2_{H^1(\Omega)} \\
&\geq \frac{\lambda}{4}||D^+_\tau U^k||^2_{L^2(\Omega)} + \frac{1}{4}|U^{k+1}|_{H^1(\Omega)} + \frac{1}{4}|U^k|^2_{H^1(\Omega)}.
\end{aligned}$$

□

Theorem 3.3.5.
Let $f \in C([0, T]; L^2(\Omega))$ be the given right-hand side of (2.17), the sequence $(\mathcal{T}_\nu)_{\nu\in\mathbb{N}}$ of decompositions of Ω be admissible, shape-regular and globally quasi uniform and the constant time step size $\tau \in (0, \frac{T}{2}]$ be given. Assume that there exists $\lambda \in (0, 2)$ such that the CFL condition holds true. Then

- ***Energy conservation***

  - *for $f = 0$, the Leapfrog method* (3.7),(3.8) *conserves energy in the sense that*
  $$\mathcal{E}_{\mathrm{LF}}^k = \mathcal{E}_{\mathrm{LF}}^0 \quad \text{for } k = 1, ..., N_t - 1$$
  - *for $f \neq 0$, the relation*
  $$\sqrt{\mathcal{E}_{\mathrm{LF}}^k} \leq \sqrt{\mathcal{E}_{\mathrm{LF}}^0} + \sum_{j=1}^{k} \frac{\tau}{\sqrt{\lambda}} ||f^j||_{L^2(\Omega)} \quad \text{for } k = 1, ..., N_t - 1$$
  holds true, where $f^j(x) = f(x, t^j), \quad x \in \Omega$.

- ***Stability*** *The Leapfrog method* (3.7),(3.8) *is stable in the sense that*
$$||D_\tau^+ U^k||_{L^2(\Omega)} + |U^{k+1}|_{H^1(\Omega)} \leq \left(\frac{1}{\sqrt{\lambda}} + 1\right) [\sqrt{2}||D_\mathcal{T}^+ U^0||_{L^2(\Omega)} + |U^0|_{H^1(\Omega)} + |U^1|_{H^1(\Omega)} + \sum_{j=1}^{k} \frac{2\tau}{\sqrt{\lambda}} ||f^j||_{L^2(\Omega)}]$$
for $k = 1, ..., N_t - 1$.

Proof. For the Energy Conservation: Let $k \in \{1, ..., N_t - 1\}$ be fixed. For $j \in \{1, ..., k\}$ choose
$$v_h = U^{j+1} - U^{j-1} = (U^{j+1} - U^j) + (U^j - U^{j-1}) \in S_{h,0}^1(\Omega).$$
By plugging it into the variational formulation (3.8), together with Lemma 3.3.4 and the Cauchy-Schwarz inequality, the relations follows, see [19, Theorem 3.2.5]).
For the stability: Estimate the norms of the left-hand side by the discrete energy, see [19, Theorem 3.2.6]. □

Theorem 3.3.6.
Let $f \in C([0, T]; L^2(\Omega))$ be the given right-hand side of (2.17)*, the sequence $(\mathcal{T}_\nu)_{\nu \in \mathbb{N}}$ of decompositions of Ω be admissible, shape-regular and globally quasi uniform and the constant time step size $\tau \in (0, \frac{T}{2}]$ be given. Assume that there exist $\lambda \in (0, 2)$ such that the CFL condition holds true. In addition, let the unique solution u of* (2.19) *satisfy $u \in C^4([0, T]; H_0^1(\Omega))$. Then, the Leapfrog method* (3.7),(3.8) *fullfils:*

- *the $L^2(\Omega)$ error estimate*
$$\max_{k=2,...,N_t} ||U^k - u(\cdot, t^k)||_{L^2(\Omega)} \leq C_P \left(\frac{1}{\sqrt{\lambda}} + 1\right) \big[\sqrt{2}||D_\tau^+(U^0 - Q_h^1 u(\cdot, t^0))||_{L^2(\Omega)} + |U^0 - Q_h^1 u_0|_{H^1(\Omega)} + |U^1 - Q_h^1 u(\cdot, t^1)|_{H^1(\Omega)} + \frac{2T}{\sqrt{\lambda}} ||Q_h^1 \partial_{tt} u - \partial_{tt} u||_{C([0,T];L^2(\Omega))} + \frac{\tau^2 C_P T}{2\sqrt{\lambda}} ||\partial_t^4 u||_{C([0,T];H_0^1(\Omega))}\big] + ||Q_h^1 u - u||_{C([0,T];L^2(\Omega))},$$

- *the $H_0^1(\Omega)$ error estimate*

$$\max_{k=2,\dots,N_t} |U^k - u(\cdot,t^k)|_{H^1(\Omega)} \leq \left(\frac{1}{\sqrt{\lambda}}+1\right)\Big[\sqrt{2}||D_\tau^+(U^0 - Q_h^1 u(\cdot,t^0))||_{L^2(\Omega)}$$
$$+ |U^0 - Q_h^1 u_0|_{H^1(\Omega)} + |U^1 - Q_h^1 u(\cdot,t^1)|_{H^1(\Omega)} + \frac{2T}{\sqrt{\lambda}}||Q_h^1\partial_{tt}u - \partial_{tt}u||_{C([0,T];L^2(\Omega))}$$
$$+ \frac{\tau^2 C_P T}{2\sqrt{\lambda}}||\partial_t^4 u||_{C([0,T];H_0^1(\Omega))}\Big] + ||Q_h^1 u - u||_{C([0,T];H_0^1(\Omega))},$$

- *the $L^2(\Omega)$ error estimate of the discrete time derivative*

$$\max_{k=1,\dots,N_t-1} ||D_\tau^+(U^k - u(\cdot,t^k))||_{L^2(\Omega)} \leq \left(\frac{1}{\sqrt{\lambda}}+1\right)\Big[\sqrt{2}||D_\tau^+(U^0 - Q_h^1 u(\cdot,t^0))||_{L^2(\Omega)}$$
$$+ |U^0 - Q_h^1 u_0|_{H^1(\Omega)} + |U^1 - Q_h^1 u(\cdot,t^1)|_{H^1(\Omega)} + \frac{2T}{\sqrt{\lambda}}||Q_h^1\partial_{tt}u - \partial_{tt}u||_{C([0,T];L^2(\Omega))}$$
$$+ \frac{\tau^2 C_P T}{2\sqrt{\lambda}}||\partial_t^4 u||_{C([0,T];H_0^1(\Omega))}\Big]$$
$$+ ||Q_h^1\partial_t u - \partial_t u||_{C([0,T];L^2(\Omega))} + \frac{\tau}{2}||Q_h^1\partial_{tt}u - \partial_{tt}u||_{C([0,T];L^2(\Omega))},$$

where $Q_h^1 : H_0^1(\Omega) \to S_{h,0}^1(\Omega)$ is the projection for $v \in H_0^1(\Omega)$:

$$\forall w_h \in S_{h,0}^1(\Omega): \quad \langle \nabla_x Q_h^1 v, \nabla_x w_h\rangle_{L^2(\Omega)} = \langle \nabla_x v, \nabla_x w_h\rangle_{L^2(\Omega)}.$$

Proof. See [19, Theorem 3.2.7]. □

Remark 3.3.7. *An energy conservation, stability and error estimate analogous to the ones in Theorem 3.3.5 and Theorem 3.3.6 holds true, if the weaker CFL condition:*

$$\exists \bar{\lambda} \in (0,4) \quad \text{such that } c_{inv}\frac{\tau}{h^2} \leq 4 - \bar{\lambda},$$

is satisfied, see [2, 19].

3.4 Crank-Nicolson Method for the Wave Equation

Let the wave speed of (2.17) be $c(x) = 1$ for all $x \in \Omega$. Let the sequence $(\mathcal{T}_\nu)_{\nu\in\mathbb{N}}$ of decompositions of Ω be admissible, shape-regular, $f \in C([0,T];L^2(\Omega))$ be the given right-hand side of (2.17), and $N_t \in \mathbb{N}, N_t \geq 2$ such that $\tau = \frac{T}{N_t} \in [0, \frac{T}{2}]$ be the constant step size with the corresponding time t^k given.

Applying the Crank-Nicolson method on the equation (2.17) with (2.17a)-(2.17c), consider the approximation on the spatial variable as in Ansatz 3.1.4:

$$U^k(x) = \sum_{i=1}^{M} a_i^k \psi_i(x) \approx u(x,t^k) \quad \text{for } x \in \Omega, k = \{0,1,...,N_t\},$$

afterwards apply the second-order central difference operator for the temporal variable, and replace

$$\nabla_x u(x,t^k) \approx \frac{1}{4}(\nabla_x U^{k+1}(x) + 2\nabla_x U^k(x) + \nabla_x U^{k-1}(x)), \quad x \in \Omega, \tag{3.12}$$

and

$$f(x,t^k) \approx \frac{1}{4}(f(x,t^{k+1}) + 2f(x,t^k) + f(x,t^{k-1})), \quad x \in \Omega, \tag{3.13}$$

see [2, 19, 32, 8].
Find a function $U^k \in S^1_{h,0}(\Omega)$ for $k = 0, 1, ..., N_t$ such that

$$U^0 = u_{0,h}, \quad U^1 = u_{1,h}$$

where $u_{0,h}$ and $u_{1,h}$ are approximations of the initial conditions (2.17b) and (2.17c):

$$u(\cdot,0) = u_0 \approx u_{0,h} \in S^1_{h,0}(\Omega), \quad u(\cdot,t^1) \approx u_{1,h} \in S^1_{h.0}(\Omega). \tag{3.14}$$

For $k = 1, 2, ..., N_t - 1$, take test function $v_h \in S^1_{h,0}(\Omega)$ multiply and integrate on the approximated wave equation (as is being done in Example 3.1.5) and together with the second-order central difference operator and (3.12),(3.13) on (2.17) gives:

$$\frac{1}{\tau^2}\langle U^{k+1} - 2U^k + U^{k-1}, v_h\rangle_{L^2(\Omega)} + \frac{1}{4}\langle \nabla_x U^{k+1} + 2\nabla_x U^k + \nabla_x U^{k-1}, \nabla_x v_h\rangle_{L^2(\Omega)} = \frac{1}{4}\langle f^{k+1} + 2f^k + f^{k-1}, v_h\rangle_{L^2(\Omega)} \tag{3.15}$$

with $f^k(x) = f(x,t^k)$ for $x \in \Omega$.
By changing $v_h = \psi_j$, $j = 1, ..., M$, the discrete variational formulation (3.15) is equivalent to solving the linear system

$$\begin{aligned} &\frac{1}{\tau^2}M_h(\underline{a}^{k+1} - 2\underline{a}^k + \underline{a}^{k-1}) + \frac{1}{4}A_h(\underline{a}^{k+1} + 2\underline{a}^k + \underline{a}^{k-1}) = \frac{1}{4}(\underline{f}^{k+1} + 2\underline{f}^k + \underline{f}^{k-1}) \\ &\Leftrightarrow (M_h + \frac{\tau^2}{4}A_h)\underline{a}^{k+1} = \frac{\tau^2}{4}(\underline{f}^{k+1} + 2\underline{f}^k + \underline{f}^{k-1}) - \frac{\tau^2}{4}A_h(2\underline{a}^k + \underline{a}^{k-1}) + M_h(2\underline{a}^k - \underline{a}^{k-1}) \end{aligned} \tag{3.16}$$

for $k = 1, ..., N_t - 1$, where $\underline{a}^k = \begin{pmatrix} a_1^k \\ ... \\ a_M^k \end{pmatrix} \in \mathbb{R}^M$, $k = 0, ..., N_t$ is the unknown coefficient vector , M_h, A_h are the mass and stiffness matrix given in (3.10) and $\underline{f}^k = \begin{pmatrix} \langle f^k, \psi_1\rangle_{L^2(\Omega)} \\ ... \\ \langle f^k, \psi_M\rangle_{L^2(\Omega)} \end{pmatrix}$, $k = 0, ..., N_t$.

Remark 3.4.1. *In every iteration, a linear system with the system matrix $M_h + \frac{\tau^2}{4}A_h$ has to be solved for $\underline{a}^{k+1}$, when $\underline{a}^k$, $\underline{a}^{k-1}$ are known. Since the mass and stiffness matrices are positive definite, see Lemma 3.3.2,* (3.16) *is uniquely solvable, hence* (3.15) *has a unique solution $U^{k+1} \in S^1_{h,0}(\Omega)$ for $k = 1, ..., N_t - 1$ when U^k, U^{k-1} are known.*

Definition 3.4.2.
Let $U^k \in S^1_{h,0}(\Omega)$ be the solution of (3.14),(3.15) *for the time steps t^k, $k = 0, 1, ..., N_t$. The discrete energy of the Crank-Nicolson method* (3.14),(3.15) *is defined by*

$$\mathcal{E}^k_{\mathrm{CN}} = \frac{1}{2}||D^+_\tau U^k||^2_{L^2(\Omega)} + \frac{1}{2}\langle \nabla_x U^{k+\frac{1}{2}}, \nabla_x U^{k+\frac{1}{2}}\rangle_{L^2(\Omega)}$$

for $k = 0, 1, ..., N_t - 1$ with the average

$$U^{k+\frac{1}{2}} = \frac{1}{2}(U^{k+1} + U^k).$$

Because $\mathcal{E}_{\mathrm{CN}}^k$ is non-negative, there is not required the CFL condition for the stability analysis on the contrary to the Leapfrog method.

Theorem 3.4.3. *Let $f \in C([0,T];L^2(\Omega))$ be a given right-hand side of (3.9), the sequence of decompositions of Ω be admissible, shape-regular and not necessarily quasi-uniform, and the constant time step size $\tau \in (0, \frac{T}{2}]$ be given. Then*

- ***Energy Conservation***
  - *for $f = 0$, the Crank-Nicolson method (3.14),(3.15) conserves energy in the sense that*
$$\mathcal{E}_{\mathrm{CN}}^k = \mathcal{E}_{\mathrm{CN}}^0 \quad \text{for } k = 1, ..., N_t - 1,$$
  - *for $f \neq 0$, the relation*
$$\sqrt{\mathcal{E}_{\mathrm{CN}}^k} \leq \sqrt{\mathcal{E}_{\mathrm{CN}}^0} + \sum_{j=1}^{k} \frac{\tau}{4\sqrt{2}} ||f^{j+1} + 2f^j + f^{j-1}||_{L^2(\Omega)}, \quad \text{for } k = 1, ..., N_t - 1.$$
- ***Stability*** *The Crank-Nicolson method (3.15),(3.16) is stable in the sense that*
$$||D_\tau^+ U^k||_{L^2(\Omega)} + |U^{k+\frac{1}{2}}|_{H^1(\Omega)} \leq 2||D_\tau^+ U^0||_{L^2(\Omega)} + 2|U^{\frac{1}{2}}|_{H^1(\Omega)} + \sum_{j=1}^{k} \frac{\tau}{2} ||f^{j+1} + 2f^j + f^{j-1}||_{L^2(\Omega)}$$
  for $k = 1, ..., N_t - 1$.

Proof. For the Energy Conservation: Let $k \in \{1, ..., N_t - 1\}$ be fixed. For $j \in \{1, ..., k\}$ choose
$$v_h = U^{j+1} - U^{j-1} = (U^{j+1} - U^j) + (U^j - U^{j-1}) = (U^{j+1} + U^j) - (U^j + U^{j-1}) \in S_{h,0}^1(\Omega).$$
By plugging it into the variational formulation (3.15), together with the discrete energy and the Cauchy-Schwarz inequality, the relations follows, see [19, Theorem 3.3.4].
For the Stability:
Let $k \in \{1, ..., N_t - 1\}$ be fixed. By using the energy conservation from above and the definition of the discrete energy it yields:
$$||D_\tau^+ U^k||_{L^2(\Omega)} + |U^{k+\frac{1}{2}}|_{H^1(\Omega)} \leq 2\sqrt{2}\Big[\sqrt{\frac{1}{2}||D_\tau^+ U^0||_{L^2(\Omega)}^2 + \frac{1}{2}|U|_{H^1(\Omega)}^{\frac{1}{2}}} + \sum_{j=1}^{k} \frac{\tau}{4\sqrt{2}} ||f^{j+1} + 2f^j + f^{j-1}||_{L^2(\Omega)}\Big]$$
So, the assertion follows, see [19, Theorem 3.3.5].

□

Remark 3.4.4. *The stability analysis only estimates the H^1 norm of the average of two consecutive time steps, which is in some sense slightly weaker than the Leapfrog method.*

Theorem 3.4.5.
Let $f \in C([0,T];L^2(\Omega))$ be a given right-hand side of (3.9), the sequence of decompositions

of Ω be admissible, shape-regular and not necessarily quasi-uniform, and the constant time step size $\tau \in (0, \frac{T}{2}]$ be given. In addition, let the unique solution u of (2.19) satisfy $u \in C^4([0,T]; H_0^1(\Omega))$. Then, the Crank-Nicolson method (3.15),(3.16) fulfils:

- *the $L^2(\Omega)$ error estimate*

$$\begin{aligned}\max_{k=1,\dots,N_t-1} ||U^{k+\frac{1}{2}} - u(\cdot, t^{k+\frac{1}{2}})||_{L^2(\Omega)} &\leq C_P\big[2||D_\tau^+(U^0 - Q_h^1 u(\cdot,t^0))||_{L^2(\Omega)} \\ &+ |U^0 - Q_h^1 u_0|_{H^1(\Omega)} + |U^1 - Q_h^1 u(\cdot,t^1)|_{H^1(\Omega)} + \tau^2 C_P T||\partial_t^4 u||_{C([0,T];H_0^1(\Omega))} \\ &+ 2T||\partial_{tt}u - Q_h^1\partial_{tt}u||_{C([0,T];L^2(\Omega))}\big] + ||Q_h^1 u - u||_{C([0,T];L^2(\Omega))} + \frac{\tau^2}{8}||\partial_{tt}u||_{C([0,T];L^2(\Omega))},\end{aligned}$$

- *the $H_0^1(\Omega)$ error estimate*

$$\begin{aligned}\max_{k=1,\dots,N_t-1} |U^{k+\frac{1}{2}} - u(\cdot, t^{k+\frac{1}{2}})|_{H^1(\Omega)} &\leq 2||D_\tau^+(U^0 - Q_h^1 u(\cdot,t^0))||_{L^2(\Omega)} \\ &+ |U^0 - Q_h^1 u_0|_{H^1(\Omega)} + |U^1 - Q_h^1 u(\cdot,t^1)|_{H^1(\Omega)} + \tau^2 C_P T||\partial_t^4 u||_{C([0,T];H_0^1(\Omega))} \\ &+ 2T||\partial_{tt}u - Q_h^1\partial_{tt}u||_{C([0,T];L^2(\Omega))} + ||Q_h^1 u - u||_{C([0,T];H_0^1(\Omega))} + \frac{\tau^2}{8}||\partial_{tt}u||_{C([0,T];H_0^1(\Omega))},\end{aligned}$$

- *the $L^2(\Omega)$ error estimate of the discrete time derivative*

$$\begin{aligned}\max_{k=1,\dots,N_t-1} ||D_\tau^+(U^k - u(\cdot,t^k))||_{L^2(\Omega)} &\leq 2||D_\tau^+(U^0 - Q_h^1 u(\cdot,t^0))||_{L^2(\Omega)} \\ &+ |U^0 - Q_h^1 u_0|_{H^1(\Omega)} + |U^1 - Q_h^1 u(\cdot,t^1)|_{H^1(\Omega)} \\ &+ \tau^2 C_P T||\partial_t^4 u||_{C([0,T];H_0^1(\Omega))} + 2T||\partial_{tt}u - Q_h^1\partial_{tt}u||_{C([0,T];L^2(\Omega))} \\ &+ ||Q_h^1\partial_t u - \partial_t u||_{C([0,T];L^2(\Omega))} + \frac{\tau}{2}||Q_h^1\partial_{tt}u - \partial_{tt}u||_{C([0,T];L^2(\Omega))},\end{aligned}$$

where $Q_h^1 : H_0^1(\Omega) \to S_{h,0}^1(\Omega)$ is the projection for $v \in H_0^1(\Omega)$:

$$\forall w_h \in S_{h,0}^1(\Omega): \quad \langle \nabla_x Q_h^1 v, \nabla_x w_h\rangle_{L^2(\Omega)} = \langle \nabla_x v, \nabla_x w_h\rangle_{L^2(\Omega)},$$

and

$$t^{k+\frac{1}{2}} = \frac{t^{k+1} + t^k}{2} = t^k + \frac{\tau}{2}, \quad k = 0, ..., N_t - 1.$$

Chapter 4

Space-Time Methods for the Wave Equation

Space-time methods are an alternative discretization of a time-dependent problem by treating the time t just as another variable and address the problem in one dimension higher. Meaning that the time variable is considered as an additional spatial variable. This ansatz may lead to structured decompositions, i.e. tensor-product approaches, see [3, 4, 12, 15], or unstructured decompositions, see [11, 22, 29], of the space-time domain Q.

4.1 Variational Formulation

Consider the homogeneous Dirichlet problem for the wave equation

$$\partial_{tt}u(x,t) - \Delta_x u(x,t) = f(x,t), \qquad (x,t) \in Q = \Omega \times (0,T), \tag{4.1}$$

$$u(x,t) = 0, \qquad (x,t) \in \Sigma = \partial\Omega \times [0,T], \tag{4.1a}$$

$$u(x,0) = \partial_t u(x,0) = 0, \qquad x \in \Omega, \tag{4.1b}$$

where $\Omega \subset \mathbb{R}^d$, $d = 1, 2, 3$, is a bounded domain with Lipschitz boundary $\partial\Omega$, $T > 0$ is the terminal time and f is the given right-hand side.
Define the Sobolev spaces

$$H^{1,1}_{0;0,}(Q) = H^1_{0,}(0,T;L^2(\Omega)) \cap L^2(0,T;H^1_0(\Omega)) \subset H^1(Q)$$

and

$$H^{1,1}_{0;,0}(Q) = H^1_{,0}(0,T;L^2(\Omega)) \cap L^2(0,T;H^1_0(\Omega)) \subset H^1(Q),$$

which are endowed with the inner product

$$\langle u, v\rangle_{H^{1,1}_{0;}(Q)} = \int_0^T \int_\Omega (\partial_t u(x,t)\partial_t v(x,t) + \nabla_x u(x,t) \cdot \nabla_x v(x,t))dxdt$$

and the induced norm

$$|u|_{H^1(Q)} = \sqrt{\langle u, u\rangle_{H^{1,1}_{0;}(Q)}} = \left\{ \int_0^T \int_\Omega (|\partial_t u(x,t)|^2 + \sum_{m=1}^d |\partial_{x_m} u(x,t)|^2)dxdt \right\}^{\frac{1}{2}}$$

with the subspaces

$$H^1_{0,}(0,T;L^2(\Omega)) = \{v \in H^1(0,T;L^2(\Omega)) \colon v(\cdot,0) = 0 \text{ in } L^2(\Omega)\} \subset C([0,T];L^2(\Omega))$$

and

$$H^1_{,0}(0,T;L^2(\Omega)) = \{v \in H^1(0,T;L^2(\Omega)):\ v(\cdot,T) = 0 \text{ in } L^2(\Omega)\} \subset C([0,T];L^2(\Omega)).$$

Remark 4.1.1. *Note that in $H^{1,1}_{0;0,}(Q)$ and $H^{1,1}_{0;,0}(Q)$, the seminorm $|\cdot|_{H^1(Q)}$ is a $||\cdot||_{H^1(Q)}$ equivalent norm due to the Poincaré inequality.*

To derive a variational formulation of (4.1) with (4.1a), (4.1b) in subspaces of $H^1(Q)$ consider

$$\int_0^T \int_\Omega \partial_{tt} u(x,t) v(x,t) dx dt + \int_0^T \int_\Omega \nabla_x u(x,t) \cdot \nabla_x v(x,t) dx dt = \int_0^T \int_\Omega f(x,t) v(x,t) dx dt \tag{4.2}$$

where $v(x,t)$ is sufficiently smooth with $v(x,T) = 0$ and $f \in L^2(Q)$ is given.
The first part of the left-hand side of (4.2) is the second-order time derivative $\partial_{tt} u(x,t)$, multiplied by the function $v(x,t) \in H^{1,1}_{0;,0}(Q)$ and integrated via the space-time cylinder Q. Integration by parts on that gives

$$\int_0^T \int_\Omega \partial_{tt} u(x,t) v(x,t) dx dt = -\int_0^T \int_\Omega \partial_t u(x,t) \partial_t v(x,t) dx dt + \int_\Omega \partial_t u(x,T) v(x,T) dx - \int_\Omega \partial_t u(x,0) v(x,0) dx$$

and further,

$$\int_0^T \int_\Omega \partial_{tt} u(x,t) v(x,t) dx dt = -\int_0^T \int_\Omega \partial_t u(x,t) \partial_t v(x,t) dx dt$$

because $v(x,T) = 0$ by definition and $\partial_t u(x,0) = 0$ by (4.1b).
So, one can define the bilinear form $a(\cdot,\cdot) : H^{1,1}_{0;0,}(Q) \times H^{1,1}_{0;,0}(Q) \to \mathbb{R}$,

$$a(u,v) = -\langle \partial_t u, \partial_t v \rangle_{L^2(Q)} + \langle \nabla_x u, \nabla_x v \rangle_{L^2(Q)}, \qquad u \in H^{1,1}_{0;0,}(Q),\ \ v \in H^{1,1}_{0;,0}(Q). \tag{4.3}$$

Lemma 4.1.2.
The bilinear form $a(\cdot,\cdot) : H^{1,1}_{0;0,}(Q) \times H^{1,1}_{0;,0}(Q) \to \mathbb{R}$ is bounded, i.e.

$$|a(u,v)| \le |u|_{H^1(Q)} |v|_{H^1(Q)}$$

for all $u \in H^{1,1}_{0;0,}(Q)$, $v \in H^{1,1}_{0;,0}(Q)$.

Proof. The assertion follows immediately from the Cauchy-Schwarz inequality. □

So, the variational formulation of (4.1) with (4.1a), (4.1b) is to find $u \in H^{1,1}_{0;0,}(Q)$ such that

$$a(u,v) = \langle f, v \rangle_{L^2(Q)} \quad \text{for all } v \in H^{1,1}_{0;,0}(Q), \tag{4.4}$$

where the right-hand side $f \in L^2(Q)$ is given. Note that, the initial condition $u(\cdot,0) = 0$ is considered in the strong sense and $\partial_t u(\cdot,0) = 0$ is incorporated in a weak sense.

Theorem 4.1.3.
Let $f \in L^2(Q)$ be given. Then, there exists a unique solution $u \in H^{1,1}_{0;0,}(Q)$ of (4.4), satisfying

$$|u|_{H^1(Q)} \le \frac{1}{\sqrt{2}} T ||f||_{L^2(Q)}.$$

Proof. For the variational formulation (4.4), there exists a unique solution $u \in H^{1,1}_{0;0,}(Q)$, see [18, Chapter IV, Theorem 3.1 and Theorem 3.2]. The estimate follows by a Fourier series ansatz as in [18, Section 7, Chapter IV], see [33, Theorem 4.2.23]. □

4.2 Space-Time Discretization: Finite Element Method

Let $\Omega \subset \mathbb{R}^d$, $d = 1, 2, 3$, be a bounded Lipschitz domain. Define the decomposition of the time interval $(0, T)$

$$0 =< t_0 < t_1 < t_2 < \cdots < t_{N_t-1} < t_{N_t} = T$$

where $N_t \in \mathbb{N}$, $N_t \geq 2$, is the time discretization parameter.
So, every time interval $\tau_l = (t_{l-1}, t_l) \subset \mathbb{R}$, has the mesh size

$$h_{t,l} = t_l - t_{l-1} \quad \text{for } l = 1, ..., N_t.$$

In addition,

$$h_t = h_{t,\max} = \max_l h_{t,l}, \quad h_{t,\min} = \min_l h_{t,l}$$

are, with respect to time, the global and minimal mesh sizes respectively.

For the spatial domain Ω, consider a shape-regular sequence $(\mathcal{T}_\nu)_{\nu\in\mathbb{N}}$ of admissible decompositions of Ω

$$\mathcal{T}_\nu = \{\omega_i \subset \mathbb{R}^d : \ i = 1, ..., N_x\}$$

into finite elements $\omega_i \subset \mathbb{R}^d$ with mesh size $h_{x,i}$, as defined in Definition 3.1.1 for $h_{\omega_i} = h_{x,i}$, $N = N_x$. For $d = 1$, the spatial elements ω_i are intervals, for $d = 2$ triangles or quadrilaterals and for $d = 3$ tetrahedra or hexahedra.

Consider, for a tensor-product ansatz, admissible decompositions

$$\overline{Q} = \overline{\Omega} \times [0, T] = \cup_{i=1}^{N_x} \overline{\omega_i} \times \cup_{l=1}^{N_t} \overline{\tau_l}$$

with $N = N_x \cdot N_t$ space-time elements.
Define the spaces of continuous piecewise multilinear functions

$$V^1_{h_x,0}(\Omega) = \operatorname{span}\{\psi_j\}_{j=1}^{M_x} \subset H^1_0(\Omega), \quad S^1_{h_t}(0, T) = \operatorname{span}\{\phi_l\}_{l=0}^{N_t} \subset H^1_0(0, T)$$

where M_x is the number of interior vertices of the decomposition of Ω, $M_x = \dim V_{h_x,0}(\Omega)$. The space $S^1_{h_t}(0, T)$ is defined as in Ansatz 3.1.4. The space $V^1_{h_x,0}(\Omega)$ is either $S^1_{h_x}(\Omega) \cap H^1_0(\Omega)$ of piecewise linear continuous functions on intervals, triangles and tetrahedra for $d = 1, 2, 3$ respectively. Or $V^1_{h_x,0}(\Omega)$ is the space $Q^1_{h_x}(\Omega) \cap H^1_0(\Omega)$ of piecewise linear/bilinear/trilinear continuous functions on intervals, quadrilaterals and hexahedra for $d = 1, 2, 3$ respectively.

4.3 Petrov-Galerkin Method for the Wave Equation

Let the decompositions of $\overline{Q}$ be admissible and $f \in L^2(Q)$ be the given right-hand side of (4.1).
Applying the Petrov-Galerkin method on the equation (4.1) with (4.1a),(4.1b), consider the

approximation $u_h \in Q_h^1(Q) \cap H_{0;0,}^{1,1}(Q)$

$$u_h(x,t) = \sum_{l=1}^{N_t} \sum_{j=1}^{M_x} u_j^l \psi_j(x) \phi_l(t) = \sum_{j=1}^{M_x} U_{h_t,j}(t) \psi_j(x), \quad U_{h_t,j}(t) = \sum_{l=1}^{N_t} u_j^l \phi_l(t)$$

for $(x,t) \in \overline{Q}$, where ϕ_l is piecewise linear continuous nodal basis function with respect to time and ψ_j is a piecewise linear/bilinear/trilinear continuous nodal basis function with respect to space. Furthermore, $U_{h_t,j} \in S_{h_t}^1(0,T)$ for $j = 1, ..., M_x$, see [33, Section 2.8] .

Take a test function $v_h \in Q_h^1(Q) \cap H_{0;,0}^{1,1}(Q)$, multiply and integrate on the approximate wave equation, gives

$$a(u_h, v_h) = \langle f, v_h \rangle_{L^2(Q)} \quad \text{for all } v_h \in Q_h^1(Q) \cap H_{0;,0}^{1,1}(Q), \tag{4.5}$$

where $u_h \in Q_h^1(Q) \cap H_{0;0,}^{1,1}(Q)$ is sought and the right-hand side $f \in L^2(Q)$ is given.
The discrete variational formulation (4.5) is equivalent to the global linear system

$$K_h \underline{u} = \underline{F} \tag{4.6}$$

with the system matrix

$$K_h = -A_{h_t} \otimes M_{h_x} + M_{h_t} \otimes A_{h_x} \in \mathbb{R}^{N_t \cdot M_x \times N_t \cdot M_x},$$

where $M_{h_x} \in \mathbb{R}^{M_x \times M_x}$ and $A_{h_x} \in \mathbb{R}^{M_x \times M_x}$ denote the spatial mass and stiffness matrices of (3.10), the temporal stiffness matrix

$$A_{h_t} = \begin{pmatrix} -\frac{1}{h_{t,1}} & & & & \\ \frac{1}{h_{t,1}} + \frac{1}{h_{t,2}} & -\frac{1}{h_{t,2}} & & & \\ -\frac{1}{h_{t,2}} & \frac{1}{h_{t,2}} + \frac{1}{h_{t,3}} & -\frac{1}{h_{t,3}} & & \\ & \ddots & \ddots & \ddots & \\ & & -\frac{1}{h_{t,N_t-1}} & \frac{1}{h_{t,N_t-1}} + \frac{1}{h_{t,N_t}} & -\frac{1}{h_{t,N_t}} \end{pmatrix} \in \mathbb{R}^{N_t \times N_t},$$

the temporal mass matrix

$$M_{h_t} = \frac{1}{6} \begin{pmatrix} h_{t,1} & & & & \\ 2h_{t,1} + 2h_{t,2} & h_{t,2} & & & \\ h_{t,2} & 2h_{t,2} + 2h_{t,3} & h_{t,3} & & \\ & \ddots & \ddots & \ddots & \\ & & h_{t,N_t-1} & 2h_{t,N_t-1} + 2h_{t,N_t} & h_{t,N_t} \end{pmatrix} \in \mathbb{R}^{N_t \times N_t}$$

and the corresponding vector $\underline{F} \in \mathbb{R}^{N_t \cdot M_x}$ of the right-hand side.

Remark 4.3.1. *The Petrov-Galerkin finite element discretization* (4.5) *can be realised as a two-step method.*

Define $\underline{u} = (\underline{U}^1, \underline{U}^2, ..., \underline{U}^{N_t})^\top$ the vector of the unknowns, where the vector $\underline{U}^I = (u_1^I, u_2^I, ..., u_{M_x}^I)^\top$ for $I = 1, ..., N_t$ corresponds to the time step t_I. Furthermore $\underline{F} = (\underline{f}^0, ..., \underline{f}^{N_t-1})^\top$ is the given right-hand side, where $\underline{f}^I = (\langle f, \psi_1 \phi^I \rangle_{L^2(Q)}, \langle f, \psi_2, \phi^I \rangle_{L^2(Q)}, \cdots, \langle f, \psi_{M_x} \phi^I \rangle_{L^2(Q)})^\top$ for

$I = 0, ..., N_t - 1$ corresponds to the time step t_I. The global linear system (4.6) becomes

$$\begin{pmatrix} \frac{1}{h_{t,1}}M_{h_x} + \frac{h_{t,1}}{6}A_{h_x} & & & & \\ -\left(\frac{1}{h_{t,1}} + \frac{1}{h_{t,2}}\right)M_{h_x} + \frac{h_{t,1}+h_{t,2}}{3}A_{h_x} & \frac{1}{h_{t,2}}M_{h_x} + \frac{h_{t,2}}{6}A_{h_x} & & & \\ B_3 & C_3 & D_3 & & \\ & \ddots & \ddots & \ddots & \\ & & B_{N_t} & C_{N_t} & D_{N_t} \end{pmatrix} \cdot \begin{pmatrix} \underline{U}^1 \\ \underline{U}^2 \\ \underline{U}^3 \\ \cdots \\ \underline{U}^{N_t} \end{pmatrix} = \begin{pmatrix} \underline{f}^0 \\ \underline{f}^1 \\ \underline{f}^2 \\ \cdots \\ \underline{f}^{N_t-1} \end{pmatrix},$$

where

$$B_l = \frac{1}{h_{t,l-1}}M_{h_x} + \frac{h_{t,l-1}}{6}A_{h_x},$$

$$C_l = -\left(\frac{1}{h_{t,l-1}} + \frac{1}{h_{t,l}}\right)M_{h_x} + \frac{h_{t,l-1} + h_{t,l}}{3}A_{h_x},$$

$$D_l = \frac{1}{h_{t,l}}M_{h_x} + \frac{h_{t,l}}{6}A_{h_x}$$

for $l = 3, \ldots, N_t$. In the first two iteration, the linear systems

$$\left[\frac{1}{h_{t,1}}M_{h_x} + \frac{h_{t,1}}{6}A_{h_x}\right]\underline{U}^1 = \underline{f}^0 \tag{4.7}$$

$$\left[\frac{1}{h_{t,2}}M_{h_x} + \frac{h_{t,2}}{6}A_{h_x}\right]\underline{U}^2 = \underline{f}^1 + \left[\left(\frac{1}{h_{t,1}} + \frac{1}{h_{t,2}}\right)M_{h_x} - \frac{h_{t,1} + h_{t,2}}{3}A_{h_x}\right]\underline{U}^1 \tag{4.8}$$

has to be solved in order to compute $\underline{U}^1$ and $\underline{U}^2$.
Then, in every iteration a linear system

$$\left[\frac{1}{h_{t,l+1}}M_{h_x} + \frac{h_{t,l+1}}{6}A_{h_x}\right]\underline{U}^{l+1} = \underline{f}^l - \left[\frac{1}{h_{t,l}}M_{h_x} + \frac{h_{t,l}}{6}A_{h_x}\right]\underline{U}^{l-1} + \left[\left(\frac{1}{h_{t,l}} + \frac{1}{h_{t,l+1}}\right)M_{h_x} - \frac{h_{t,l} + h_{t,l+1}}{3}A_{h_x}\right]\underline{U}^l \tag{4.9}$$

has to be solved for $\underline{U}^{l+1}$, when $\underline{U}^l$, $\underline{U}^{l-1}$ are known for $l = 2, ..., N_t - 1$.

Remark 4.3.2. *Since the mass matrix M_{h_x} and the stiffness matrix A_{h_x} are positive definite, see Lemma 3.3.2, the linear systems* (4.7), (4.8) *and* (4.9) *are uniquely solvable, thus the global linear system* (4.6) *is uniquely solvable, hence* (4.5) *has a unique solution $u_h \in Q_h^1(Q) \cap H_{0;0,}^{1,1}(Q)$.*

Remark 4.3.3. *Let a uniform time mesh size $h_t > 0$. In order to prove, in a certain sense, stability and relate error estimates of* (4.5)*, see [33, page 156-158], it needs to determine the CFL condition*

$$h_t < \sqrt{\frac{12}{c_{inv}}}h_x \tag{4.10}$$

with the inverse inequality constant c_{inv} with respect to the spatial mesh, see Lemma 3.1.7.

Example 4.3.4. *For the one-dimensional case, it holds true that $c_{inv} = 12$, see page 23-24, so the stability of* (4.5) *follows for the CFL condition*

$$h_t < h_x.$$

Remark 4.3.5. *Let $\Omega = (0, L_1) \times \cdots \times (0, L_d)$ with uniform mesh sizes $h_{x_1}, ..., h_{x_d}$. So, $V_{h_x,0} \subset H_0^1(\Omega)$ is of tensor-product structure*

$$V_{h_x,0}(\Omega) = (S_{h_{x_1}}(0, L_1) \otimes \cdots \otimes S_{h_{x_d}}(0, L_d)) \cap H_0^1(\Omega).$$

Then, one concludes that $c_{inv} = 12d$.
Therefore, the stability holds for the CFL condition

$$h_t < \frac{h_{x,\min}}{\sqrt{d}}.$$

4.3.1 Comparison of the Petrov-Galerkin Method with the Newmark Method

Let the pointwise in time variational formulation of (4.1) with (4.1a), (4.1b) as in Theorem 2.4.4 of Section 2.4, i.e. for almost all $t \in (0, T)$, there is

$$\forall v \in H_0^1(\Omega): \quad \langle \partial_{tt} u(\cdot, t), v\rangle_\Omega + \langle \nabla_x u(\cdot, t), \nabla_x v\rangle_{L^2(\Omega)} = \langle f(\cdot, t), v\rangle_{L^2(\Omega)}, \tag{4.11}$$

$$u(x, 0) = \partial_t u(x, 0) = 0 \quad \text{for } x \in \Omega \tag{4.11a}$$

with the unique solution $u \in C^0([0, T]; H_0^1(\Omega)) \cap C^1([0, T]; L^2(\Omega))$ for a given right-hand side $f \in C([0, T]; L^2(\Omega))$.
Consider a discretisation of a tensor-product type as in Section 4.2 with the finite-dimensional space $Q_h^1(Q) = V_{h_x,0}^1(\Omega) \otimes S_{h_t}^1(0, T)$. Therefore, introduce for $x \in \Omega$ the approximations

$$u_h(x, t) = \sum_{l=1}^{N_t} \sum_{j=1}^{M_x} u_j^l \psi_j(x) \phi_l(t) = \sum_{l=1}^{N_t} U_{h_x,l}(x) \phi_l(t) \simeq u(x, t),$$

$$\hat{u}_h(x, t) = \sum_{l=1}^{N_t} \sum_{j=1}^{M_x} \hat{u}_j^l \psi_j(x) \phi_l(t) = \sum_{l=1}^{N_t} \hat{U}_{h_x,l}(x) \phi_l(t) \simeq \partial_t u(x, t),$$

with

$$U_{h_x,l}(x) = \sum_{j=1}^{M_x} u_j^l \psi_j(x) \simeq u(x, t_l),$$

$$\hat{U}_{h_x,l}(x) = \sum_{j=1}^{M_x} \hat{u}_j^l \psi_j(x) \simeq \partial_t u(x, t_l),$$

where u_j^l, $\hat{u}_j^l$ are the unknown coefficients of $U_{h_x,l}$, $\hat{U}_{h_x,l} \in V_{h_x,0}^1(\Omega)$ for $l \in \{0, ..., N_t\}$.
A semi-discrete approximation as in Section 3.1 can be defined as follows. For each $t \in [0, T]$ look for a function $u_h(\cdot, t) \in V_{h_x,0}^1(\Omega)$ that satisfies

$$\forall v_{h_x} \in V_{h_x,0}^1(\Omega): \quad \langle \partial_{tt} u_h(\cdot, t), v_{h_x}\rangle_\Omega + \langle \nabla_x u_h(\cdot, t), \nabla_x v_{h_x}\rangle_{L^2(\Omega)} = \langle f(\cdot, t), v_{h_x}\rangle_{L^2(\Omega)}, \tag{4.12}$$

$$u_h(x, 0) = \partial_t u_h(x, 0) = 0 \quad \text{for } x \in \Omega. \tag{4.12a}$$

Ansatz 4.3.6.

Consider the simple ordinary differention equation of second-order in time

$$\begin{aligned} y''(t) &= g(t, y(t), y'(t)), \quad t \in (0,T), \\ y(0) &= 0, \\ y'(0) &= 0, \end{aligned}$$

where $g : [0,T] \to \mathbb{R} \times \mathbb{R} \times \mathbb{R}$ is a continuous functions. Divide [0,T] as in Section 4.2. Denote y^n the approximation of $y(t_n)$, the Newmark method generates the sequence: set $y^0 = 0$, $z^0 = 0$ and compute

$$y^{n+1} = y^n + h_{t,n} z^n + (h_{t,n})^2 [\beta g_{n+1} + (\frac{1}{2} - \beta) g_n], \tag{4.13}$$

$$z^{n+1} = z^n + h_{t,n} [\gamma g_{n+1} + (1-\gamma) g_n] \tag{4.13a}$$

for $n = 0, ..., N_t - 1$, where β and γ are non-negative parameters, and $g_n = g(t_n, y^n, z^n)$ with z^n is an approximation of $y'(t_n)$.
The condition $\gamma \geq \frac{1}{2}$ is necessary for the stability of the method. Moreover, if $\beta = \frac{1}{4}$ and $\gamma = \frac{1}{2}$ the Newmark method is unconditionally stable. For long time integration, it is preferable to use the condition $\beta \geq \frac{(\gamma + \frac{1}{2})^2}{4}$ for suitable $\gamma \geq \frac{1}{2}$, see [26, Section 8.6/8.7].

For the pointwise in time variational formulation (4.11) with (4.11a), a conforming discretization in space with $V_{h_x,0}(\Omega) \subset H_0^1(\Omega)$ in combination with the Newmark scheme as in Ansatz 4.3.6 leads to find the functions $U_{h_x,l}, \hat{U}_{h_x,l} \in V^1_{h_x,0}(\Omega)$ for $l \in \{0, ..., N_t\}$ such that

$$U_{h_x,0} = 0, \qquad \hat{U}_{h_x,0} = 0 \tag{4.14}$$

and for $l = 1, ..., N_t$

$$\begin{aligned} \frac{1}{h_{t,l}^2} \langle U_{h_x,l} - U_{h_x,l-1} - h_{t,l} \hat{U}_{h_x,l-1}, v_{h_x} \rangle_{L^2(\Omega)} + \langle \beta \nabla_x U_{h_x,l} + (\frac{1}{2} - \beta) \nabla_x U_{h_x,l-1}, \nabla_x v_{h_x} \rangle_{L^2(\Omega)} \\ = \langle \beta f^l + (\frac{1}{2} - \beta) f^{l-1}, v_{h_x} \rangle_{L^2(\Omega)} \end{aligned} \tag{4.15}$$

for all $v_{h_x} \in V^1_{h_x,0}(\Omega)$ and

$$\begin{aligned} \frac{1}{h_{t,l}} \langle \hat{U}_{h_x,l} - \hat{U}_{h_x,l-1}, \hat{v}_{h_x} \rangle_{L^2(\Omega)} + \langle \gamma \nabla_x U_{h_x,l} + (1-\gamma) \nabla_x U_{h_x,l-1}, \nabla_x \hat{v}_{h_x} \rangle_{L^2(\Omega)} \\ = \langle \gamma f^l + (1-\gamma) f^{l-1}, \hat{v}_{h_x} \rangle_{L^2(\Omega)} \end{aligned} \tag{4.16}$$

for all $\hat{v}_{h_x} \in V^1_{h_x,0}(\Omega)$, where $f^l \in L^2(\Omega)$, $f^l(x) = f(x, t_l)$, see [26, 6, 7, 17].
The Newmark method (4.14),(4.15), (4.16) is equivalent to the linear systems

$$\underline{U}^0 = 0, \qquad \underline{\hat{U}}^0 = 0 \tag{4.17}$$

and for all $l = 1, ..., N_t$

$$\frac{1}{h_{t,l}^2} M_{h_x} [\underline{U}^l - \underline{U}^{l-1} - h_{t,l} \underline{\hat{U}}^{l-1}] + A_{h_x} [\beta \underline{U}^l + (\frac{1}{2} - \beta) \underline{U}^{l-1}] = \beta \underline{f}^l + (\frac{1}{2} - \beta) \underline{f}^{l-1} \tag{4.18}$$

$$\frac{1}{h_{t,l}} M_{h_x} [\underline{\hat{U}}^l - \underline{\hat{U}}^{l-1}] + A_{h_x} [\gamma \underline{U}^l + (1-\gamma) \underline{U}^{l-1}] = \gamma \underline{f}^l + (1-\gamma) \underline{f}^{l-1} \tag{4.19}$$

where $M_{h_x} \in \mathbb{R}^{M_x \times M_x}$ and $A_{h_x} \in \mathbb{R}^{M_x \times M_x}$ denote the spatial mass and stiffness matrices of (3.10), $\underline{u} = (\underline{U}^1, ..., \underline{U}^{N_t})^\top$, $\underline{\hat{u}} = (\underline{\hat{U}}^1, ..., \underline{\hat{U}}^{N_t})^\top$ are the vectors of the unknowns and $\underline{F} = (\underline{f}^0, ..., \underline{f}^{N_t - 1})^\top$ is the given right-hand side as defined in page 36.

To transfer the Newmark method (4.18), (4.19) with two unknowns into a scheme with only one unknown, it needs to compute (4.18) in time $l+1$ and l

$$\frac{1}{h_{t,l+1}}M_{h_x}[\underline{U}^{l+1}-\underline{U}^{l}]-M_{h_x}\hat{\underline{U}}^{l}+h_{t,l+1}A_{h_x}[\beta\underline{U}^{l+1}+(\frac{1}{2}-\beta)\underline{U}^{l}]=h_{t,l+1}\beta\underline{f}^{l+1}$$
$$+h_{t,l+1}(\frac{1}{2}-\beta)\underline{f}^{l} \quad (4.20)$$

$$\frac{1}{h_{t,l}}M_{h_x}[\underline{U}^{l}-\underline{U}^{l-1}]-M_{h_x}\hat{\underline{U}}^{l-1}+h_{t,l}A_{h_x}[\beta\underline{U}^{l}+(\frac{1}{2}-\beta)\underline{U}^{l-1}]=h_{t,l}\beta\underline{f}^{l}+h_{t,l}(\frac{1}{2}-\beta)\underline{f}^{l-1}. \quad (4.20a)$$

By subtracting (4.20a) from (4.20) together with (4.19) gives

$$M_{h_x}\left[\frac{1}{h_{t,l+1}}\underline{U}^{l+1}-(\frac{1}{h_{t,l+1}}+\frac{1}{h_{t,l}})\underline{U}^{l}+\frac{1}{h_{t,l}}\underline{U}^{l-1}\right]$$
$$+A_{h_x}\left[h_{t,l+1}\beta\underline{U}^{l+1}+(\frac{h_{t,l+1}}{2}-h_{t,l+1}\beta-h_{t,l}\beta+h_{t,l}\gamma)\underline{U}^{l}+(h_{t,l}\beta-\frac{h_{t,l}}{2}+h_{t,l}-h_{t,l}\gamma)\underline{U}^{l-1}\right]=$$
$$h_{t,l+1}\beta\underline{f}^{l+1}+(\frac{h_{t,l+1}}{2}-h_{t,l+1}\beta-h_{t,l}\beta+h_{t,l}\gamma)\underline{f}^{l}+(h_{t,l}\beta-\frac{h_{t,l}}{2}+h_{t,l}-h_{t,l}\gamma)\underline{f}^{l-1} \quad (4.21)$$

for $l=1,...,N_t-1$, and

$$\frac{1}{h_{t,1}^2}M_{h_x}\underline{U}^{1}+A_{h_x}\beta\underline{U}^{1}=\beta\underline{f}^{1}+(\frac{1}{2}-\beta)\underline{f}^{0}. \quad (4.22)$$

Then, in every iteration the linear system

$$\left[\frac{1}{h_{t,l+1}}M_{h_x}+h_{t,l+1}\beta A_{h_x}\right]\underline{U}^{l+1}=$$
$$h_{t,l+1}\beta\underline{f}^{l+1}+(\frac{h_{t,l+1}}{2}-h_{t,l+1}\beta-h_{t,l}\beta+h_{t,l}\gamma)\underline{f}^{l}+(h_{t,l}\beta-\frac{h_{t,l}}{2}+h_{t,l}-h_{t,l}\gamma)\underline{f}^{l-1}+$$
$$\left[(\frac{1}{h_{t,l+1}}+\frac{1}{h_{t,l}})M_{h_x}-(\frac{h_{t,l+1}}{2}-h_{t,l+1}\beta-h_{t,l}\beta+h_{t,l}\gamma)A_{h_x}\right]\underline{U}^{l}-$$
$$\left[\frac{1}{h_{t,l}}M_{h_x}+(h_{t,l}\beta-\frac{h_{t,l}}{2}+h_{t,l}-h_{t,l}\gamma)A_{h_x}\right]\underline{U}^{l-1} \quad (4.23)$$

has to be solved for $\underline{U}^{l+1}$, when $\underline{U}^{l}$, $\underline{U}^{l-1}$ are known for $l=1,...,N_t-1$.

Theorem 4.3.7. *By choosing the Newmark parameters $\beta=\frac{1}{6}$ and $\gamma=\frac{1}{2}$, the linear systems of Petrov-Galerkin method* (4.9) *and Newmark method* (4.20) *are the same, when ignoring the terms with the right-hand side f.*

Remark 4.3.8. *By choosing the Newmark parameters $\beta=0$, $\gamma=\frac{1}{2}$ and uniform time mesh size, the linear system* (4.23) *becomes*

$$M_{h_x}\underline{U}^{l+1}=h_{t,l}^2\underline{f}^{l}+[2M_{h_x}-A_{h_x}h_{t,l}^2]\underline{U}^{l}-M_{h_x}\underline{U}^{l-1} \quad (4.24)$$

for $l=1,\cdots,N_t-1$ with

$$\underline{U}^{0}=0, \quad (4.24a)$$

$$M_{h_x}\underline{U}^{1}=\frac{h_{t,1}^2}{2}\underline{f}^{0}. \quad (4.24b)$$

The method (4.24), (4.24a),(4.24b) *is the Leapfrog Method of Section 3.3, see* (3.9).

The matrix M_{h_x} is positive definite, see Lemma 3.3.2, and hence the linear systems (4.24), (4.24b) *are uniquely solvable for all $l = 1, ..., N_t - 1$. Stability, error estimates and a conservation of a discrete energy holds true with a CFL condition, see Theorem 3.3.5 and Theorem 3.3.6*

Remark 4.3.9. *By choosing the Newmark parameters $\beta = \frac{1}{4}$, $\gamma = \frac{1}{2}$ and uniform time mesh size, the linear system* (4.23) *becomes*

$$\big[M_{h_x} + \frac{h_{t,l}^2}{4} A_{h_x}\big]\underline{U}^{l+1} = \big[2M_{h_x} - \frac{h_{t,l}^2}{2} A_{h_x}\big]\underline{U}^{l} - \big[M_{h_x} + \frac{h_{t,l}^2}{4} A_{h_x}\big]\underline{U}^{l-1} + \frac{h_{t,l}^2}{2}\big(\frac{\underline{f}^{l+1}}{2} + \underline{f}^{l} + \frac{\underline{f}^{l-1}}{2}\big) \quad (4.25)$$

for $l = 1, \cdots, N_t - 1$ with

$$\underline{U}^0 = 0 \quad (4.25a)$$

$$\big[M_{h_x} + \frac{h_{t,1}^2}{4} A_{h_x}\big]\underline{U}^1 = \frac{h_{t,1}^2}{4}\big(\underline{f}^1 - \underline{f}^0\big). \quad (4.25b)$$

The method (4.25), (4.25a),(4.25b) *is the Crank-Nicolson Method of Section 3.4, see* (3.16). *The matrix $M_{h_x} + \frac{h_{t,l}^2}{4} A_{h_x}$ is positive definite, see Lemma 3.3.2, and hence the linear systems* (4.25), (4.25b) *are uniquely solvable for all $l = 1, ..., N_t - 1$. Stability of* (4.18),(4.19) *for $\beta = \frac{1}{4}$, $\gamma = \frac{1}{2}$ holds true without any CFL condition because it is unconditionally stable, see Theorem 3.4.3 and [26]. Error estimates of $||u(\cdot, t_l) - U_{h_x,l}||_{L^2(\Omega)}$ for each $l = 0, ..., N_t$ are of optimal order $\mathcal{O}(h_t^2 + h_x^2)$, see Theorem 3.4.5 and [26, 6, 7]. The scheme fulfils a conservation of a discrete energy, see Theorem 3.4.3 and [26].*

Chapter 5

Numerical Results

In this Chapter the results of the numerical tests will be presented. The methods are implemented in MATLAB.
For the spatial domain mesh, *DistMesh - A Simple Mesh Generator in MATLAB* is used (Figure 5.1), see [24].

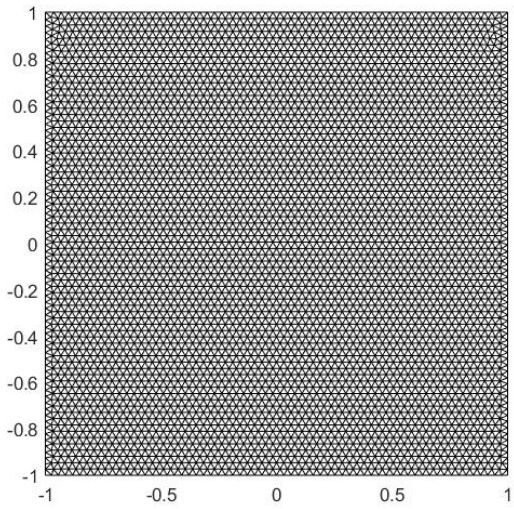

Figure 5.1: A globally quasi-uniform mesh on the square $(-1,1)^2$ with uniform mesh size $h = 2^{-5}$.

5.1 Numerical Results for the Leapfrog Method

As a spatial domain and time interval

$$\Omega = (-1,1) \times (-1,1) \quad \text{and} \quad (0,T) = (0,10)$$

are used for the numerical examples with exact solution

$$u_A(x,y,t) = (1-x^2)(1-y^2)\sin(xyt)t,$$
$$u_B(x,y,t) = (1-x^2)(1-y^2)\sin(xt)\sin(yt), \tag{5.1}$$

the corresponding right-hand sides f_A, f_B and homogeneous Dirichlet boundary conditions. The uniform spatial mesh size and the constant time step is given by

$$h_x = \frac{1}{C_x}, \quad C_x \in \mathbb{N} \quad \text{and} \quad \tau = \frac{10}{N_t}, \quad N_t \in \mathbb{N}.$$

In Table 5.1, Table 5.2, Table 5.3 and Table 5.4, the L^2-error and H^1-error for the solutions u_A, u_B are given for the Leapfrog method (3.7), (3.8) with initialization (5.1) when a refinement strategy is applied for the temporal and spatial discretizations, i.e. C_x and N_t are doubled in every refinement step. Furthermore, all the appearing integrals that are needed to compute the initialization (5.1) and the right-hand sides are calculated with higher-order quadrature rules.

In Table 5.1 and Table 5.3, one observers that the ratio between the spatial mesh size h_x and time step size τ is

$$\frac{\tau}{h_x} = 0.5656,$$

the error in L^2 is decreasing by the factor $\frac{1}{4}$, i.e. quadratic convergence, and the error in H^1 is decreasing by the factor $\frac{1}{2}$, i.e. linear convergence. Hence, the Leapfrog method is stable for these cases and the error estimates of Theorem 3.3.6 are confirmed, (Figure 5.3, Figure 5.6). Additionally, in Figure 5.2 and Figure 5.5, there are the plots of the solutions in time $t = 10$ for the last refinement step.

In Table 5.2 and Table 5.4, one observes that the error in L^2 and the error in H^1 are increasing, instead of decreasing. This is happening due to the violation of the CFL condition (3.11), where the ratio between the spatial and temporal mesh size is

$$\frac{\tau}{h_x} = 1.2567,$$

(Figure 5.4 and Figure 5.7).

Hence, the Leapfrog method is not stable for these cases.

h	τ	$\max_k \|\|\cdot\|\|_{L^2(\Omega)}$	eoc	$\max_k \|\|\cdot\|\|_{H^1(\Omega)}$	eoc
0.1768	0.1	4.1710	-	36.6267	-
0.0854	0.05	1.5336	1.3761	21.8924	0.7078
0.0422	0.025	0.4029	1.8939	11.3852	0.9264
0.0210	0.0125	0.1001	1.9948	5.7039	0.9902
0.0104	0.0063	0.0245	1.9998	2.8247	0.9986
0.0052	0.0031	0.0060	2.0038	1.4035	1.0015

Table 5.1: Numerical results for the Leapfrog method (3.7), (3.8) with refinement for the solution u_A, where the CFL condition ($\frac{\tau}{h_x} = 0.5656$) is satisfied.

h	τ	$\max_k \|\| \cdot \|\|_{L^2(\Omega)}$	eoc	$\max_k \|\| \cdot \|\|_{H^1(\Omega)}$	eoc
0.1768	0.2222	4.1714	-	36.6265	-
0.0854	0.1111	1.5333	1.3764	21.8923	0.7078
0.0422	0.0556	5.2220e+37	-122.4510	1.9627e+39	-123.8224
0.0210	0.0278	1.1668e+103	-215.5708	8.9443e+104	-216.5919
0.0104	0.0139	Inf	-Inf	Inf	-Inf

Table 5.2: Numerical results for the Leapfrog method (3.7), (3.8) with refinement for the solution u_A, where the CFL condition ($\frac{\tau}{h_x} = 1.2567$) is violated.

h	τ	$\max_k \|\| \cdot \|\|_{L^2(\Omega)}$	eoc	$\max_k \|\| \cdot \|\|_{H^1(\Omega)}$	eoc
0.1768	0.1	0.5169	-	7.9225	-
0.0854	0.05	0.3958	0.3671	6.1433	0.3498
0.0422	0.025	0.1205	1.6854	3.4728	0.8082
0.0210	0.0125	0.0311	1.9397	1.7796	0.9579
0.0104	0.0063	0.0076	1.9975	0.8841	0.9940
0.0052	0.0031	0.0019	2.0067	0.4398	1

Table 5.3: Numerical results for the Leapfrog method (3.7), (3.8) with refinement for the solution u_B, where the CFL condition ($\frac{\tau}{h_x} = 0.5656$) is satisfied.

h	τ	$\max_k \|\| \cdot \|\|_{L^2(\Omega)}$	eoc	$\max_k \|\| \cdot \|\|_{H^1(\Omega)}$	eoc
0.1768	0.2222	0.5167	-	7.9231	-
0.0854	0.1111	0.3958	0.3665	6.1433	0.3499
0.0422	0.0556	5.2312e+37	-124.3723	1.9661e+39	-125.6255
0.0210	0.0278	1.1673e+103	-215.5689	8.9482e+104	-216.5900
0.0104	0.0139	Inf	-Inf	Inf	-Inf

Table 5.4: Numerical results for the Leapfrog method (3.7), (3.8) with refinement for the solution u_B, where the CFL condition ($\frac{\tau}{h_x} = 1.2567$) is violated.

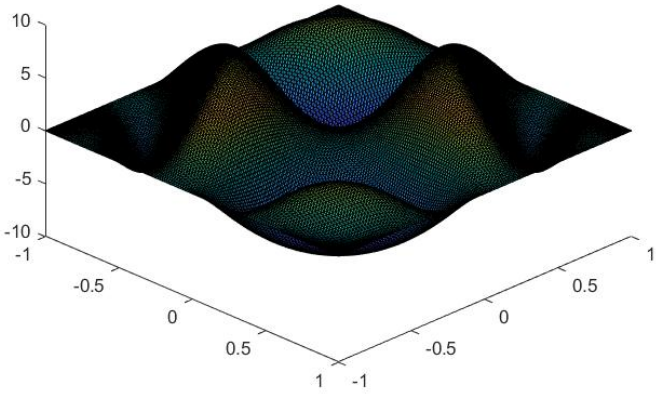

Figure 5.2: Plot of the solution u_A in time $t = 10$ for the last refinement step, i.e. $h_x = 0,0052$.

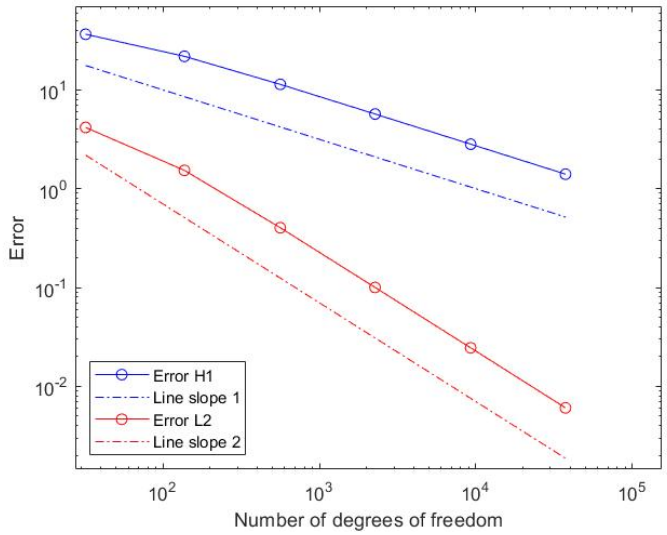

Figure 5.3: Plot of the L^2-error and H^1-error for the solution u_A, where the CFL condition ($\frac{\tau}{h_x} = 0.5656$) is satisfied.

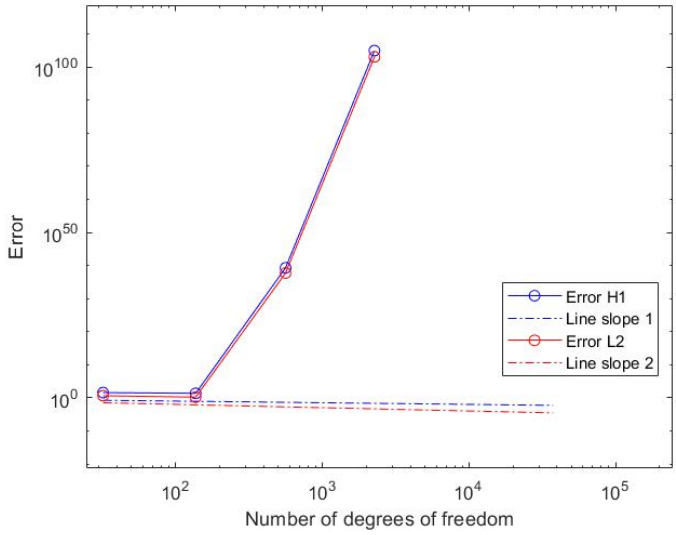

Figure 5.4: Plot of the L^2-error and H^1-error for the solution u_A, where the CFL condition ($\frac{\tau}{h_x} = 1.2567$) is violated.

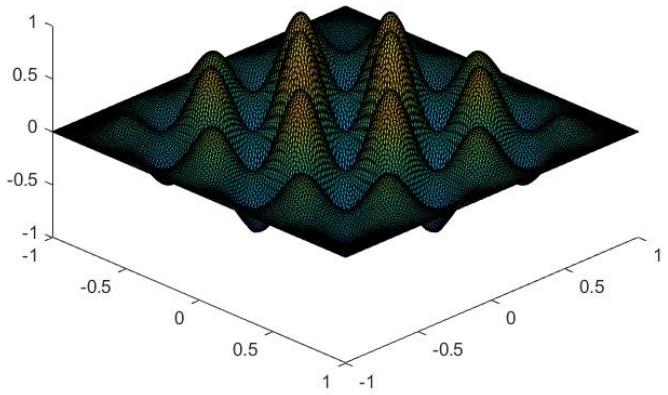

Figure 5.5: Plot of the solution u_B in time $t = 10$ for the last refinement step, i.e. $h_x = 0,0052$.

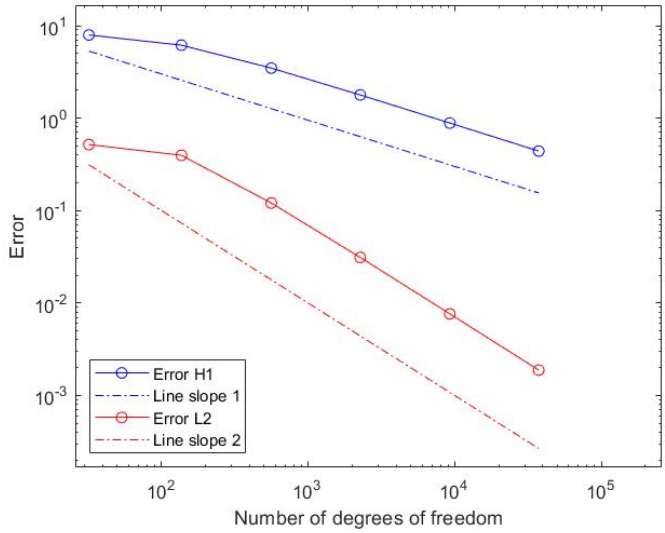

Figure 5.6: Plot of the L^2-error and H^1-error for the solution u_B, where the CFL condition ($\frac{\tau}{h_x} = 0.5656$) is satisfied.

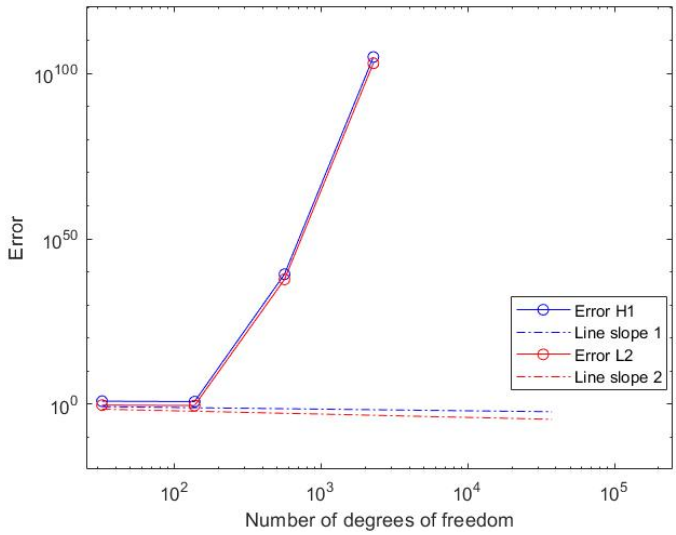

Figure 5.7: Plot of the L^2-error and H^1-error for the solution u_B, where the CFL condition ($\frac{\tau}{h_x} = 1.2567$) is violated.

5.2 Numerical Results for the Crank-Nicolson Method.

The same numerical examples as for the Leapfrog method in Section 5.1 are investigated. As a spatial domain and time interval

$$\Omega = (-1,1) \times (-1,1) \quad \text{and} \quad (0,T) = (0,10)$$

are used for the numerical examples with exact solution

$$\begin{aligned} u_A(x,y,t) &= (1-x^2)(1-y^2)\sin(xyt)t, \\ u_B(x,y,t) &= (1-x^2)(1-y^2)\sin(xt)\sin(yt), \end{aligned} \tag{5.1}$$

the corresponding right-hand sides f_A, f_B and homogeneous Dirichlet boundary conditions. The uniform spatial mesh size and the constant time step is given by

$$h_x = \frac{1}{C_x}, \quad C_x \in \mathbb{N} \quad \text{and} \quad \tau = \frac{10}{N_t}, \quad N_t \in \mathbb{N}.$$

In Table 5.5, Table 5.6, Table 5.7 and Table 5.8, the L^2-error and H^1-error for the solutions u_A, u_B are given for the Crank-Nicolson method (3.15), (3.16) with initialization (5.1) when a refinement strategy is applied for the temporal and spatial descretizations, i.e. C_x and N_t are doubled in every refinement step. Furthermore, all the appearing integrals that are needed to compute the initialization (5.1) and the right-hand sides are calculated with higher-order quadrature rules.

In Table 5.5 and Table 5.7, one observes that the ratio between the spatial mesh size h_x and time step size τ is

$$\frac{\tau}{h_x} = 0.5656,$$

the error in L^2 is decreasing by the factor $\frac{1}{4}$, i.e. quadratic convergence, and the error in H^1 is decreasing by the factor $\frac{1}{2}$, i.e. linear convergence. Hence, the Crank-Nicolson method is stable and the error estimates of Theorem 3.4.5 are confirmed, (Figure 5.9, Figure 5.12). Additionally, in Figure 5.8 and Figure 5.11 there are the plots of the solutions in time $t = 10$ for the last refinement step.

In Table 5.6 and Table 5.8, one observes that the ratio between the spatial mesh size h_x and time step size τ is

$$\frac{\tau}{h_x} = 1.2567,$$

the error in L^2 is decreasing by the factor $\frac{1}{4}$, i.e. quadratic convergence, and the error in H^1 is decreasing by the factor $\frac{1}{2}$, i.e. linear convergence. Hence, the Crank-Nicolson method is stable even on the same cases where the Leapfrog method is not (Figure 5.10, Figure 5.13), see Table 5.2, Table 5.4, Figure 5.4 and Figure 5.7.

h	τ	$\max_k \|\|\cdot\|\|_{L^2(\Omega)}$	eoc	$\max_k \|\|\cdot\|\|_{H^1(\Omega)}$	eoc
0.1768	0.1	4.1708	-	36.6269	-
0.0854	0.05	1.5336	1.3760	21.8924	0.7078
0.0422	0.025	0.4029	1.8939	11.3852	0.9264
0.0210	0.0125	0.1001	1.9948	5.7039	0.9902
0.0104	0.0063	0.0245	1.9998	2.8247	0.9986
0.0052	0.0031	0.0060	2.0038	1.4035	1.0015

Table 5.5: Numerical results for the Crank-Nicolson method (3.15), (3.16) with refinement for the solution u_A with ratio $\frac{\tau}{h_x} = 0.5656$.

h	τ	$\max_k \|\|\cdot\|\|_{L^2(\Omega)}$	eoc	$\max_k \|\|\cdot\|\|_{H^1(\Omega)}$	eoc
0.1768	0.2222	4.1710	-	36.6268	-
0.0854	0.1111	1.5337	1.3759	21.8924	0.7078
0.0422	0.0556	0.4029	1.8941	11.3852	0.9264
0.0210	0.0278	0.1001	1.9948	5.7039	0.9902
0.0104	0.0139	0.0245	1.9998	2.8247	0.9986
0.0052	0.0069	0.0060	2.0038	1.4035	1.0015

Table 5.6: Numerical results for the Crank-Nicolson method (3.15), (3.16) with refinement for the solution u_A with ratio $\frac{\tau}{h_x} = 1.2567$.

h	τ	$\max_k \|\|\cdot\|\|_{L^2(\Omega)}$	eoc	$\max_k \|\|\cdot\|\|_{H^1(\Omega)}$	eoc
0.1768	0.1	0.5171	-	7.9223	-
0.0854	0.05	0.3958	0.3676	6.1433	0.3498
0.0422	0.025	0.1205	1.6854	3.4728	0.8082
0.0210	0.0125	0.0311	1.9397	1.7796	0.9579
0.0104	0.0063	0.0076	1.9975	0.8841	0.9940
0.0052	0.0031	0.0019	2.0067	0.4398	1

Table 5.7: Numerical results for the Crank-Nicolson method (3.15), (3.16) with refinement for the solution u_B with ratio $\frac{\tau}{h_x} = 0.5656$.

h	τ	$\max_k \|\|\cdot\|\|_{L^2(\Omega)}$	eoc	$\max_k \|\|\cdot\|\|_{H^1(\Omega)}$	eoc
0.1768	0.2222	0.5171	-	7.9230	-
0.0854	0.1111	0.3958	0.3675	6.1433	0.3499
0.0422	0.0556	0.1205	1.6854	3.4728	0.8082
0.0210	0.0278	0.0311	1.9397	1.7796	0.9579
0.0104	0.0139	0.0076	1.9975	0.8841	0.9940
0.0052	0.0069	0.0019	2.0067	0.4398	1

Table 5.8: Numerical results for the Crank-Nicolson method (3.15), (3.16) with refinement for the solution u_B with ratio $\frac{\tau}{h_x} = 1.2567$.

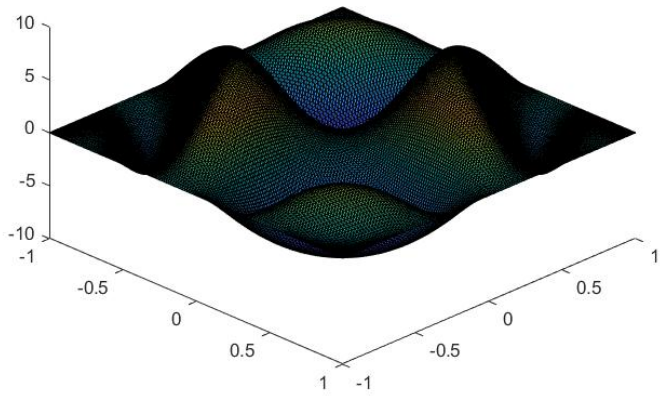

Figure 5.8: Plot of the solution u_A in time $t = 10$ for the last refinement step, i.e. $h_x = 0,0052$.

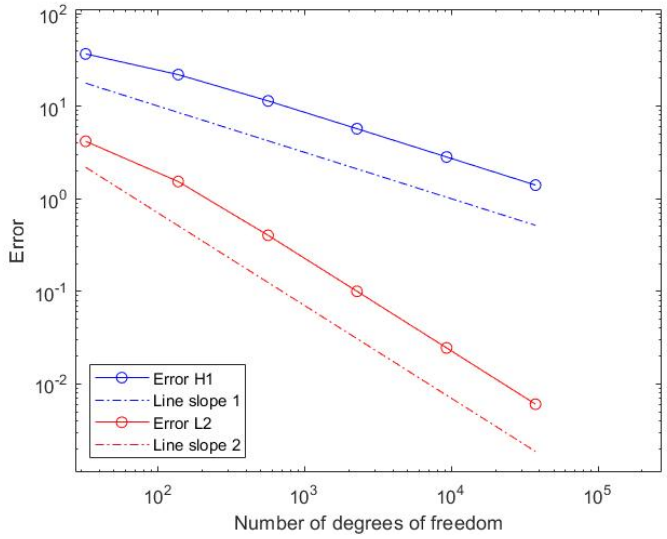

Figure 5.9: Plot of the L^2-error and H^1-error for the solution u_A with ratio $\frac{\tau}{h_x} = 0.5656$.

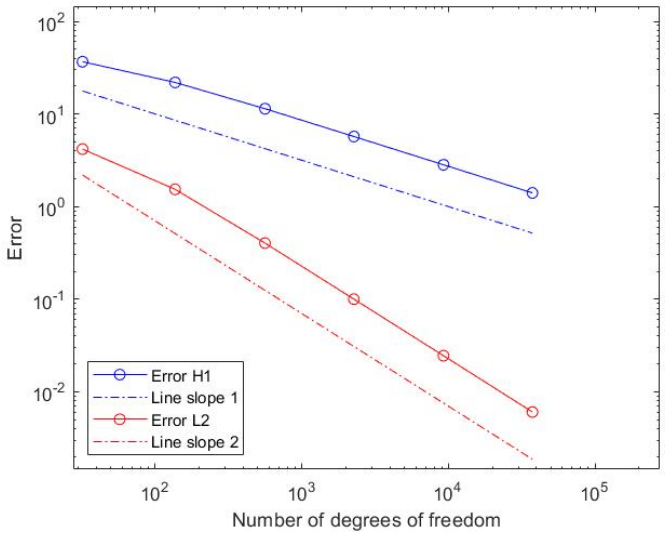

Figure 5.10: Plot of the L^2-error and H^1-error for the solution u_A with ratio $\frac{\tau}{h_x} = 1.2567$.

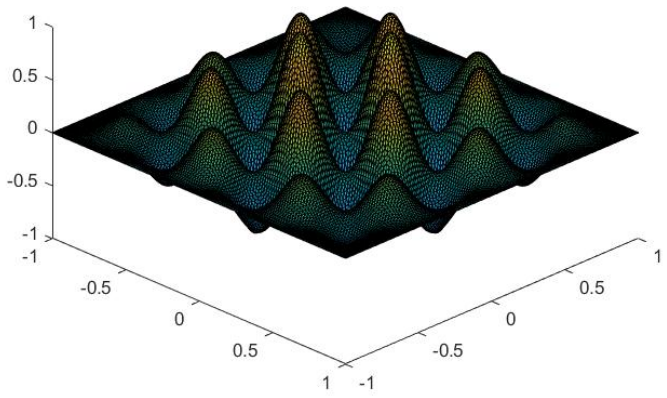

Figure 5.11: Plot of the solution u_B in time $t = 10$ for the last refinement step, i.e. $h_x = 0,0052$.

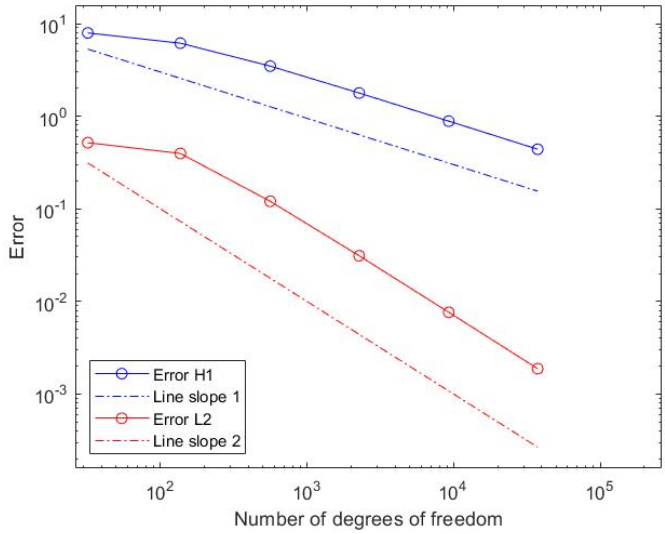

Figure 5.12: Plot of the L^2-error and H^1-error for the solution u_B with ratio $\frac{\tau}{h_x} = 0.5656$.

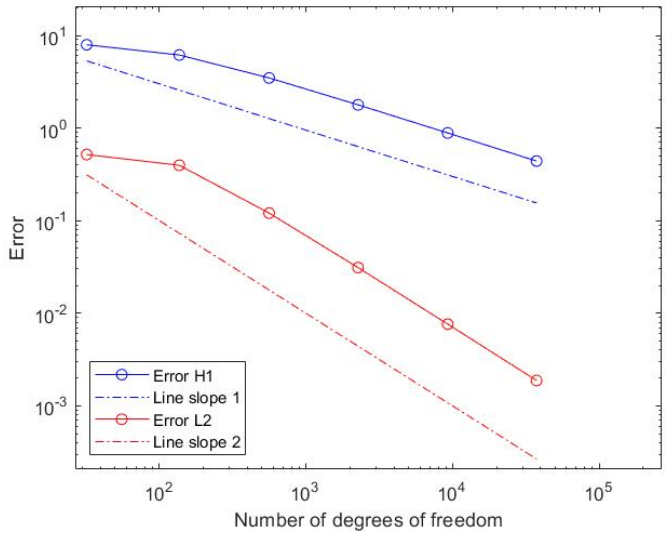

Figure 5.13: Plot of the L^2-error and H^1-error for the solution u_B with ratio $\frac{\tau}{h_x} = 1.2567$.

5.3 Numerical Results for the Petrov-Galerkin Method

The same numerical examples as for the Leapfrog method in Section 5.1 and the Crank-Nicolson method in Section 5.2 are investigated.

As a spatial domain and time interval

$$\Omega = (-1,1) \times (-1,1) \quad \text{and} \quad (0,T) = (0,10)$$

are used for the numerical examples with exact solution

$$\begin{aligned} u_A(x,y,t) &= (1-x^2)(1-y^2)\sin(xyt)t, \\ u_B(x,y,t) &= (1-x^2)(1-y^2)\sin(xt)\sin(yt), \end{aligned} \tag{5.1}$$

the corresponding right-hand sides f_A, f_B and homogeneous Dirichlet boundary conditions. The uniform spatial mesh size and the constant time step is given by

$$h_x = \frac{1}{C_x}, \quad C_x \in \mathbb{N} \quad \text{and} \quad \tau = \frac{10}{N_t}, \quad N_t \in \mathbb{N}.$$

In Table 5.9, Table 5.10, Table 5.11, Table 5.12, Table 5.13 and Table 5.14, the L^2-error and H^1-error for the solutions u_A, u_B are given for the Petrov-Galerkin method (4.7), (4.8), (4.9) with initialization (5.1) when a refinement strategy is applied for the temporal and spatial descretizations, i.e. C_x and N_t are doubled in every refinement step. Furthermore, all the appearing integrals that are needed to compute the initialization (5.1) and the right-hand sides are calculated with higher-order quadrature rules.

In Table 5.9 and Table 5.12, one observes that the ratio between the spatial mesh size h_x and time step size τ is

$$\frac{\tau}{h_x} = 0.5656,$$

the error in L^2 is decreasing by the factor $\frac{1}{4}$, i.e. quadratic convergence, and the error in H^1 is decreasing by the factor $\frac{1}{2}$, i.e. linear convergence. Hence, the Petrov-Galerkin method is stable (Figure 5.15, Figure 5.19), in the same sense as in Leapfrog and Crank-Nicolson methods, see Table 5.1, Table 5.3, Table 5.5 and Table 5.7. Additionally, in Figure 5.14 and Figure 5.18 there are the plots of the solutions in time $t = 10$ for the last refinement step.

In Table 5.10 and Table 5.13, one observes that the ratio between the spatial mesh size h_x and time step size τ is

$$\frac{\tau}{h_x} = 1.2567,$$

the error in L^2 is decreasing by the factor $\frac{1}{4}$, i.e. quadratic convergence, and the error in H^1 is decreasing by the factor $\frac{1}{2}$, i.e. linear convergence. Hence, the Petrov-Galerkin method is stable (Figure 5.16, Figure 5.20), in the same sense as in the Crank-Nicolson method, see Table 5.5, Table 5.7, Figure 5.9 and Figure 5.12. In these cases, the Leapfrog method is not stable, see Table 5.2, Table 5.4, Figure 5.4 and Figure 5.7.

In Table 5.11 and Table 5.14, one observes that the error in L^2 and the error in H^1 is increasing, instead of decreasing. This is happening due to the violation of the CFL condition (4.10), where the ratio between the spatial and temporal mesh size is

$$\frac{\tau}{h_x} = 2.2624,$$

(Figure 5.17 and Figure 5.21).
Hence, the Petrov-Galerkin method is not stable for these cases.

Remark 5.3.1. *One can observe that the Petrov-Galerkin method is stable even when the time step size is larger, i.e. less computational cost, than required for the Leapfrog method.*

h	τ	$\max_k \|\| \cdot \|\|_{L^2(\Omega)}$	eoc	$\max_k \|\| \cdot \|\|_{H^1(\Omega)}$	eoc
0.1768	0.1	4.1707	-	36.6269	-
0.0854	0.05	1.5336	1.3759	21.8924	0.7078
0.0422	0.025	0.4029	1.8940	11.3852	0.9264
0.0210	0.0125	0.1001	1.9948	5.7039	0.9902
0.0104	0.0063	0.0245	1.9998	2.8247	0.9986
0.0052	0.0031	0.0060	2.0038	1.4035	1.0015

Table 5.9: Numerical results for the Petrov-Galerkin method (4.7), (4.8), (4.9) with refinement for the solution u_A where the CFL condition ($\frac{\tau}{h_x} = 0.5656$) is satisfied.

h	τ	$\max_k \|\| \cdot \|\|_{L^2(\Omega)}$	eoc	$\max_k \|\| \cdot \|\|_{H^1(\Omega)}$	eoc
0.1768	0.2222	4.1713	-	36.6265	-
0.0854	0.1111	1.5335	1.3762	21.8924	0.7078
0.0422	0.0556	0.4029	1.8939	11.3852	0.9264
0.0210	0.0278	0.1001	1.9948	5.7039	0.9902
0.0104	0.0139	0.0245	1.9998	2.8247	0.9986
0.0052	0.0069	0.0060	2.0038	1.4035	1.0015

Table 5.10: Numerical results for the Petrov-Galerkin method (4.7), (4.8), (4.9) with refinement for the solution u_A where the CFL condition ($\frac{\tau}{h_x} = 1.2567$) is satisfied.

h	τ	$\max_k \|\| \cdot \|\|_{L^2(\Omega)}$	eoc	$\max_k \|\| \cdot \|\|_{H^1(\Omega)}$	eoc
0.1768	0.4	4.1706	-	36.6269	-
0.0854	0.2	1.5691	1.3440	22.6129	0.6633
0.0422	0.1	2.7641e+11	-36.6904	1.0389e+13	-38.0486
0.0210	0.05	1.996e+35	-77.9742	9.1955e+36	-78.9953
0.0104	0.025	2.2428e+83	-157.9345	3.4891e+85	-158.9403
0.0052	0.0125	Inf	-Inf	Inf	-Inf

Table 5.11: Numerical results for the Petrov-Galerkin method (4.7), (4.8), (4.9) with refinement for the solution u_A where the CFL condition ($\frac{\tau}{h_x} = 2,2624$) is violated.

h	τ	$\max_k \|\|\cdot\|\|_{L^2(\Omega)}$	eoc	$\max_k \|\|\cdot\|\|_{H^1(\Omega)}$	eoc
0.1768	0.1	0.5172	-	7.9220	-
0.0854	0.05	0.3958	0.3677	6.1433	0.3497
0.0422	0.025	0.1205	1.6854	3.4728	0.8082
0.0210	0.0125	0.0311	1.9397	1.7796	0.9579
0.0104	0.0063	0.0076	1.9975	0.8841	0.9940
0.0052	0.0031	0.0019	2.0067	0.4398	1

Table 5.12: Numerical results for the Petrov-Galerkin method (4.7), (4.8), (4.9) with refinement for the solution u_B where the CFL condition ($\frac{\tau}{h_x} = 0.5656$) is satisfied.

h	τ	$\max_k \|\|\cdot\|\|_{L^2(\Omega)}$	eoc	$\max_k \|\|\cdot\|\|_{H^1(\Omega)}$	eoc
0.1768	0.2222	0.5169	-	7.9238	-
0.0854	0.1111	0.3958	0.3670	6.1433	0.350
0.0422	0.0556	0.1205	1.6854	3.4728	0.8082
0.0210	0.0278	0.0311	1.9397	1.7796	0.9579
0.0104	0.0139	0.0076	1.9975	0.8841	0.9940
0.0052	0.0069	0.0019	2.0067	0.4398	1

Table 5.13: Numerical results for the Petrov-Galerkin method (4.7), (4.8), (4.9) with refinement for the solution u_B where the CFL condition ($\frac{\tau}{h_x} = 1.2567$) is satisfied.

h	τ	$\max_k \|\|\cdot\|\|_{L^2(\Omega)}$	eoc	$\max_k \|\|\cdot\|\|_{H^1(\Omega)}$	eoc
0.1768	0.4	0.5172	-	7.9220	-
0.0854	0.2	0.5069	0.0278	8.2240	-0.0514
0.0422	0.1	2.7790e+11	-38.2992	1.0445e+13	-39.4894
0.0210	0.05	1.1996e+35	-77.9666	9.1958e+36	-78.9876
0.0104	0.025	2.2428e+83	-157.9345	3.4892e+85	-158.9403
0.0052	0.0125	Inf	-Inf	Inf	-Inf

Table 5.14: Numerical results for the Petrov-Galerkin method (4.7), (4.8), (4.9) with refinement for the solution u_B where the CFL condition ($\frac{\tau}{h_x} = 2.2624$) is violated.

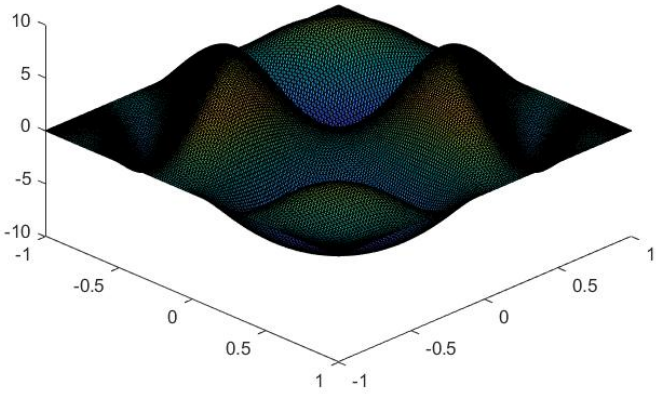

Figure 5.14: Plot of the solution u_A in time $t = 10$ for the last refinement step, i.e. $h_x = 0,0052$.

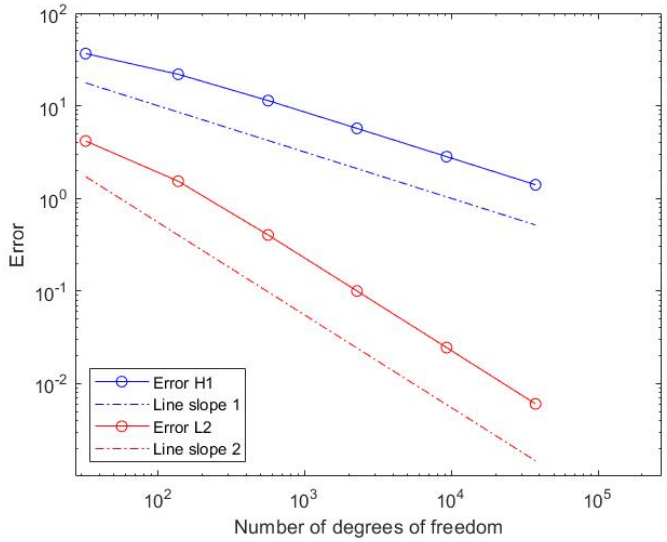

Figure 5.15: Plot of the L^2-error and H^1-error for the solution u_A, where the CFL condition ($\frac{\tau}{h_x} = 0.5656$) is satisfied.

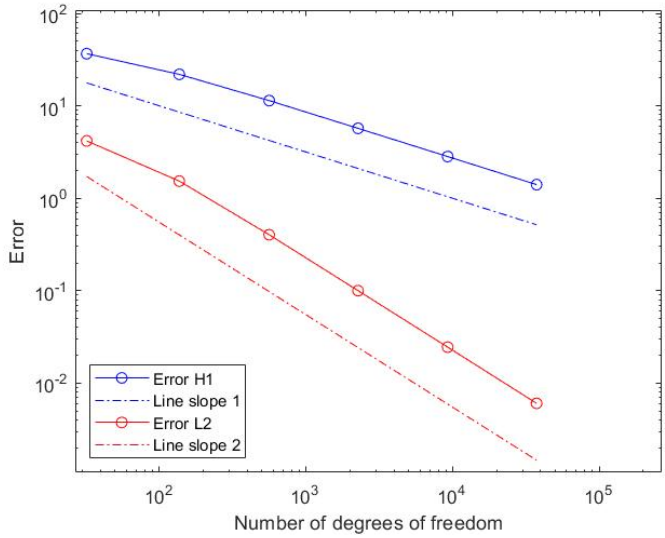

Figure 5.16: Plot of the L^2-error and H^1-error for the solution u_A, where the CFL condition ($\frac{\tau}{h_x} = 1.2567$) is satisfied.

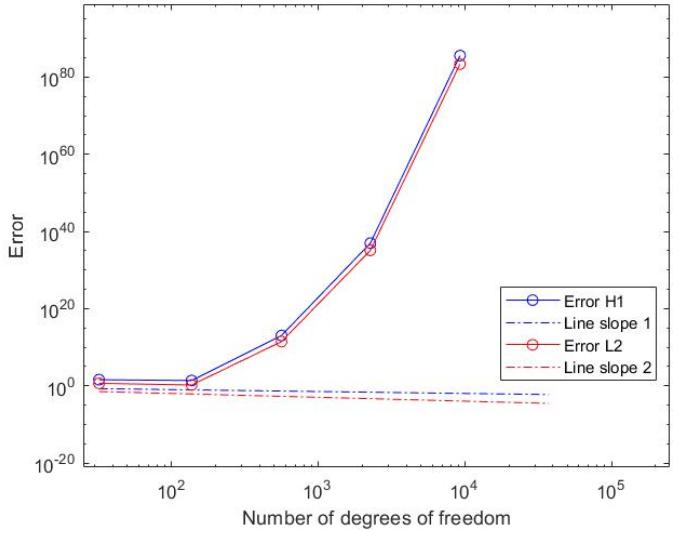

Figure 5.17: Plot of the L^2-error and H^1-error for the solution u_A, where the CFL condition ($\frac{\tau}{h_x} = 2.2624$) is violated.

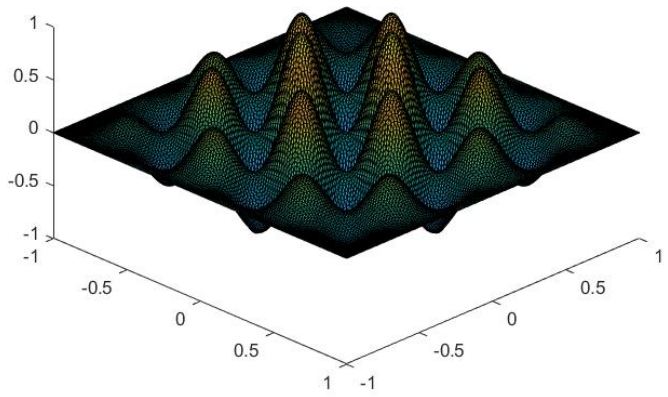

Figure 5.18: Plot of the solution u_B in time $t = 10$ for the last refinement step, i.e. $h_x = 0,0052$.

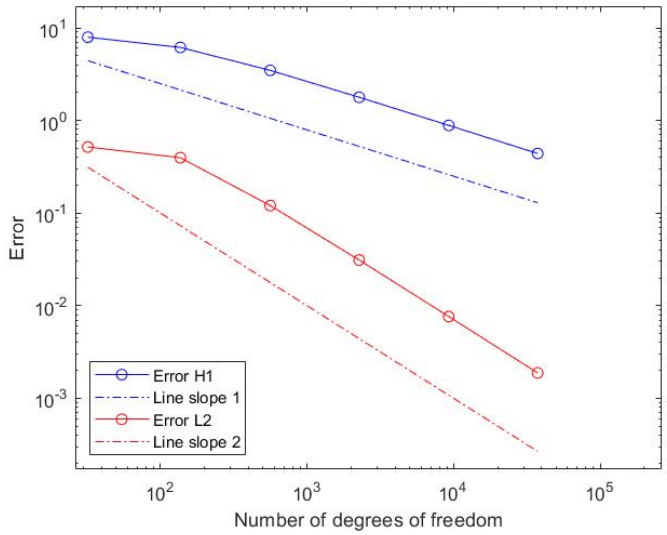

Figure 5.19: Plot of the L^2-error and H^1-error for the solution u_B, where the CFL condition ($\frac{\tau}{h_x} = 0.5656$) is satisfied.

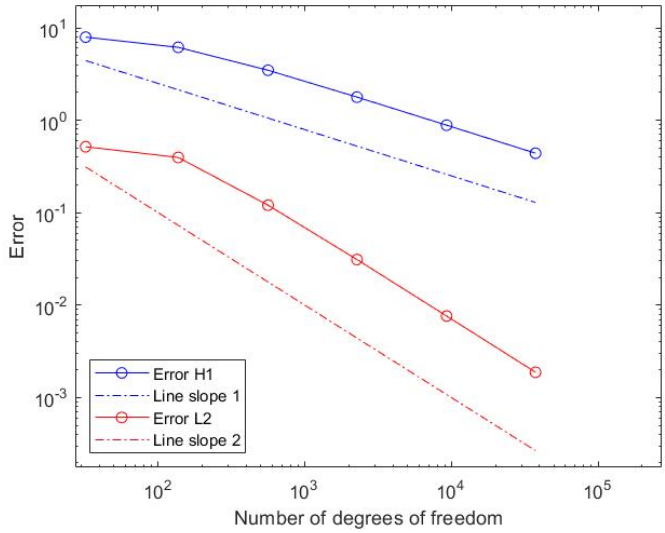

Figure 5.20: Plot of the L^2-error and H^1-error for the solution u_B, where the CFL condition ($\frac{\tau}{h_x} = 1.2567$) is satisfied.

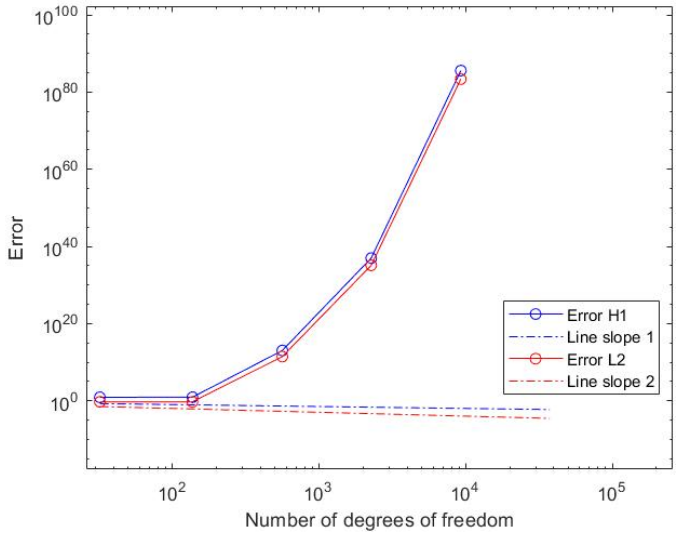

Figure 5.21: Plot of the L^2-error and H^1-error for the solution u_B, where the CFL condition ratio ($\frac{\tau}{h_x} = 2.2624$) is violated.

5.4 Comparison of the Numerical Results

The numerical results of the previous sections show that the Newmark scheme (4.22), (4.23) can be used to recast different methods to approximate solutions of the wave equation, i.e. Leapfrog, Crank-Nicolson, Petrov-Galerkin, according to the different choices of the Newmark parameters.

The decomposition of the spatial domain $\Omega = (-1, 1) \times (-1, 1)$ is admissible, shape-regular and quasi-uniform and a constant time step size $\tau \in (0, \frac{T}{2}]$ is being used, when $T = (0, 10)$. The exact solutions (5.1) with the corresponding right-hand sides $f_A \in C([0, T]; L^2(\Omega))$, $f_B \in C([0, T]; L^2(\Omega))$ and homogeneous Dirichlet boundary conditions have been investigated.

Remark 5.4.1. *The Crank-Nicolson method does not require a CFL condition for stability on the contrary to Leapfrog and Petrov-Galerkin methods, see Section 3.4.*

For the case, when the ration between the spatial mesh size h_x and the time step size τ is

$$\frac{\tau}{h_x} = 0.5656,$$

the CFL conditions (3.11) of Leapfrog and (4.10) of Petrov-Galerkin methods are satisfied, meaning that both are stable. The Crank-Nicolson method is unconditionally stable, see Remark 5.4.1. Thus, in this case, all three methods are converging and producing the same absolute L^2-errors and H^1-errors, see Table 5.1, Table 5.3, Table 5.5, Table 5.7, Table 5.9 and Table 5.12.

For the case, when the ratio is

$$\frac{\tau}{h_x} = 1,2567,$$

the CFL condition (3.11) of the Leapfrog method is violated, thus it is not stable. The absolute errors are increasing and the method is not converging, see Table 5.2 and Table 5.4. The CFL condition (4.10) of the Petrov-Galerkin method is satisfied, meaning that it is stable. The Crank-Nicolson method is unconditionally stable, see Remark 5.4.1. Hence, two of the methods are converging and producing the same absolute L^2-errors and H^1-errors, see Table 5.6, Table 5.8, Table 5.10 and Table 5.13.

Remark 5.4.2. *The Petrov-Galerkin method is stable for larger time step sizes, i.e. less computational cost, than required for the Leapfrog method.*

For the Petrov-Galerkin method, the case when the ratio is

$$\frac{\tau}{h_x} = 2.2624,$$

has also been investigated. The CFL condition (4.10) is violated, thus it is not stable. The absolute errors are increasing and the method is not converging, see Table 5.11 and Table 5.14.
In this case, the Leapfrog method would not converge either, since its CFL condition (3.11) would be violated.
On the contrary, the Crank-Nicolson method would be stable, see Remark 5.4.1. Thus, it would converge.

Chapter 6

Conclusion & Outlook

In this thesis, a second-order linear hyperbolic initial boundary value problem with variable wave speed, that depends on spatial variables in a continuous way, has been considered. For the purpose of the thesis, the theory of function spaces, and initial and boundary conditions have been introduced.

First, the general solution of the one-dimensional wave equation, by using d'Alembert's method, is derived. Furthermore, the variational formulation of the initial boundary value problem for the wave equation (2.17) with (2.17a), (2.17b), (2.17c) has been derived and ensured that the continuous problem (2.19) with (2.19a), (2.19b), (2.19c) is well-posed, by showing that it has indeed a unique solution in $C([0,T];H_0^1(\Omega))$, see Theorem 2.4.4.

Thereafter, a spatial discretization by applying the finite element method, in the finite dimensional space $S_{h,0}^1(\Omega) \subset H_0^1(\Omega)$ and a temporal discretization by applying the second-order central difference operator is used. The use of the Leapfrog method, for the discretizations of the initial boundary value problem leads to a conditionally stable method, where a CFL condition is required for stability, and the use of Crank-Nicolson method leads to an unconditionally stable method.

The discretization of the Laplace operator and of the temporal variable on the right-hand side $f \in C([0,T];L^2(\Omega))$ is what differentiate the two methods. The reason why the Crank-Nicolson method does not require a CFL condition for its stability, on the contrary with the Leapfrog method, is because it leads to a non-negative discrete energy. But this stability is only in terms of the H^1 norm of the average of two consecutive time steps, which in some sense is slightly weaker than the stability of the Leapfrog method.

Furthermore, a space-time variational formulation of the homogeneous Dirichlet problem for the wave equation (4.1) with (4.1a), (4.1b) has been derived and well-posedness is ensured by showing that the model (4.4) has a unique solution in a subspace of the Sobolev space $H^1(Q)$.

A tensor-product discretization in the space-time domain Q, by applying a space-time finite element method in the finite dimensional subspace $Q_h(Q) = V_{h_x,0}^1(\Omega) \times S_{h_t}^1(0,T) \subset H_0^1(Q)$

is derived. The use of it on the presented space-time variational formulation leads to a conditionally stable method where a CFL condition is required.

In addition, a pointwise in time variational formulation of (4.1) with (4.1a), (4.1b) as in Section 2.4 and a tensor-product type discretization, as in Section 4.2, in combination with the Newmark scheme, leads to the scheme (4.22), (4.23), that can describe all the above-mentioned methods by choosing the correct Newmark parameters β and γ, when ignoring the terms corresponding to the right-hand side f.

By implementing the Newmark scheme (4.22), (4.23) in MATLAB, numerical results for all the aforementioned methods, i.e. Leapfrog, Crank-Nicolson, Petrov-Galerkin, on a spatial domain $\Omega \subset \mathbb{R}^2$ were presented in Chapter 5. By comparing the results, one can see that the CFL of the Petrov-Galerkin method is weaker than Leapfrog method's one, whereas the Crank-Nicolson method remain stable for any given time step $\tau \in (0, \frac{T}{2}]$. Further, all methods, on their stable cases, are producing the same absolute L^2 and H^1 errors.

As a perspective, a first goal would be to perform numerical experiments for the Petrov-Galerkin method on not necessarily uniform meshes in time. This would be important, for instance, in case of exact solution with limited regularity. It would also be interesting to run the simulations presented above in a 3D spatial domain and compare the stability results.

A major achievement would be to develop an a posteriori error estimator, which then would allow to use adaptive mesh refinement, leading to a space-time Adaptive Finite Element Method (AFEM). Other future goals would be to extend the obtained results to other problems, for instance to a non-linear hyperbolic problems and eddy current problems, which arises in physics and engineering.

Bibliography

[1] R. A. Adams and J. J. F. Fournier. Sobolev Spaces. *2nd edition, Academic Press, New York*, 2003.

[2] W. Arendt and K. Urban. Partielle Differenzialgleichungen. Eine Einfuehrung in analytische und numerische Methoden. *2nd edition Berlin: Springer Spektrum,*, 2018.

[3] L. Bales and I. Lasiecka. Continuous finite elements in space and time for the nonhomogeneous wave equation. *Comput. Math Appl. 27*, pages 91–102, 3 1994.

[4] W. Bangerth, M. Geiger, and R. Rannacher. Adaptive Galerkin finite element methods for the wave equation. *Comput. Methods Appl. Math. 10*, 1 2010.

[5] E. Bazhlekova and I. Dimovski. Explicit solution for a wave equation with nonlocal condition. *AIP Conference Proceedings*, 1497:221–232, 01 2012.

[6] A. Bradji. Note on a new high order piecewise linear finite element approximation for the wave equation in one dimensional space. In Numerical analysis and its applications. *6th international conference, NAA 2016, Lozenetz, Bulgaria. Revised selected papers. Cham: Springer, 2017, pp. 235–242*, June 15–22, 2016.

[7] A. Bradji and J. Fuhrmann. Some new error estimates for finite element methods for second order hyperbolic equations using the Newmark method. *Math.Bohem. 139, 125–136*, 2 (2014).

[8] P. Chatzipantelidis and M. Plexousakis. Αριθμητική επίλυση μερικών διαφορικών εξισώσεων. *[ebook] Athens: Hellenic Academic Libraries Link*, 2015.

[9] R. Dautray and J.-L. Lions. Mathematical analysis and numerical methods for science and technology. *Springer-Verlag, Berlin,*, Vol. 5., 1992. Evolution problems. I, With the collaboration of Michel Artola, Michel Cessenat and Hélène Lanchon, Translated from the French by Alan Craig.

[10] M. Dobrowolski. Angewandte Funktionalanalysis. *2 ed. Springer-Verlag Berlin Heidelberg*, 2010.

[11] W. Dörfler, S. Findeisen, and C. Wieners. Space-time discontinuous Galerkin discretizations for linear first-order hyperbolic evolution systems. *Comput. Methods Appl. Math. 16*, pages 409–428, 3 2016.

[12] D. French and T. E. Peterson. A continuous space-time finite element method for the wave equation. *Math. Comp. 65*, pages 491–506, 214 1996.

[13] P. L. Frey, P.CJ. George. Mesh generation. Application to finite elements. *Hermes Science Publishing, Oxford, UK,*, 2000.

[14] T. Hytönen, J. Van Neerven, M. Veraar, and L. Weils. Analysis in Banach spaces. Volume I. Martingales and Littlewood-Paley theory. *Cham: Springer*, vol.63, 2016.

[15] C. Johnson. Discontinuous Galerkin finite element methods for second order hyperbolic problems. *Comput. Methods Appl. Mech. Eng. 107*, pages 117–129, 1-2 1993.

[16] P. Joly. Variational Methods for Time-dependent Wave Propagation Problems. In: Ainsworth M., Davies P., Duncan D., Rynne B., Martin P. (eds) Topics in Computational Wave Propagation. Lecture Notes in Computational Science and Engineering. *Springer, Berlin, Heidelberg*, vol 31, 2003.

[17] U. Köcher and M. Bause. Variational space-time methods for the wave equation. *J. Sci. Comput. 61, 424–453*, 2 (2014).

[18] O. A. Ladyzhenskaya. The boundary value problems of mathematical physics, vol. 49 of Applied Mathematical Sciences. *Springer-Verlag, New York*, 1985.

[19] A.B. Longva. Finite element solutions to the wave equation in non-convex domains - A relaxation of the CFL condition in the presence of local mesh refinement. *Master thesis, NTNU, Trondheim*, 2017.

[20] F. Mahmoudian and G. F. Margrave. A review of the finite-element method in seismic wave modelling. *CREWES Research Report*, 15, 2003.

[21] S. A. Migórski, A. Ochal, and Sofonea M. Nonlinear inclusions and hemivariational inequalities. *vol. 26 of Advances in Mechanics and Mathematics. Springer, New York*, 2013. Models and analysis of contact problems.

[22] A. Moiola and I. Perugia. A space-time Trefftz discontinuous Galerkin method for the acoustic wave equation in first-order formulation. *Numer. Math. 138*, pages 389–435, 2 2018.

[23] A. Novozhilov. Undergraduate course on partial differential equations. *North Dakota State University*, 2016.

[24] P.-O. Persson and G. Strang. A Simple Mesh Generator in MATLAB. *SIAM Review, Volume 46 (2), pp. 329-345*, June 2004.

[25] E. Pontiki. Αριθμητική επίλυση υπερβολικών μερικών διαφορικών εξισώσεων, εφαρμογή της μεθόδου πεπερασμένων διαφορών στην κυματική εξίσωση. *Master thesis, Technological Educational Institute of Crete, Rethymno,*, June, 2006.

[26] P.A. Raviart and J.M. Thomas. Introduction à l'analyse numérique deséquations aux dérivées partielles. *Masson*, 1983.

[27] M. Reed and B. Simon. Methods of modern mathematical physics. I. *second ed. Academic Press, New York*, 1980.

[28] B. Schweizer. Partielle Differentialgleichungen. Eine anwendungsorientierte Einführung. *Heidelberg: Springer Spektrum*, 2018.

[29] P. E. Sepúlveda Salas. Spacetime Numerical Techniques for the Wave and Schrödinger Equations. *PhD thesis, Portland State University*, 2018.

[30] C. Sogge. Lectures on nonlinear wave equations. *International Press*, 2008.

[31] O. Steinbach. Numerical Approximation Methods for Elliptic Boundary Value Problems. *Springer-Verlag New York*, 2008.

[32] O. Zafeiriou. Μελέτη ηχομείωσης θορύβου με πεπερασμένα στοιχεία. *Master thesis, Technical University of Crete*, 2015.

[33] M. Zank. Inf–sup stable space–time methods for time–dependent partial differential equations. *volume 36 of Monographic Series TU Graz: Computation in Engineering and Science*, Feb. 2020.

[34] E. Zeidler. Nonlinear functional analysis and its applications. *II/A. Spinger-Verlag, New York*, 1990.